Trends in Analytical Chemistry 173 (2024) 117655

Contents lists available at ScienceDirect

Trends in Analytical Chemistry

journal homepage: www.elsevier.com/locate/trac

Exploring advanced materials: Harnessing the synergy of inverse gas chromatography and artificial vision intelligence

Praveen Kumar Basivi [a], Tayssir Hamieh [b,c], Vijay Kakani [d], Visweswara Rao Pasupuleti [e,f], G. Sasikala [f], Sung Min Heo [g], Kedhareswara Sairam Pasupuleti [h], Moon-Deock Kim [h], Venkata Subbaiah Munagapati [i], Nadavala Siva Kumar [k], Jet-Chau Wen [i,j], Chang Woo Kim [l,*]

[a] Pukyong National University Industry-University Cooperation Foundation, Pukyong National University, Busan, 48513, Republic of Korea
[b] Faculty of Science and Engineering, Maastricht University, P.O. Box 616, 6200, MD, Maastricht, Netherlands
[c] Laboratory of Materials, Catalysis, Environment and Analytical Methods Laboratory (MCEMA), Faculty of Sciences, Lebanese University, Hadath, Lebanon
[d] Department of Integrated System Engineering, INHA University, 100 Inha-ro, Namgu, 22212, Incheon, Republic of Korea
[e] Center for International Relations and Research Collaborations and School of Applied Sciences, REVA University, Rukmini Knowledge Park, Kattigenahalli, Yelahanka, Bangalore, Karnataka, 560064, India
[f] School of Computer Sciences and Applications, REVA University, Kattigenahalli, Rukmini Knowledge Park Bangalore, 560064, India
[g] Department of Smart Green Technology Engineering, Pukyong National University, Busan, 48513, Republic of Korea
[h] Institute of Quantum Systems (IQS), Chungnam National University, 99 Daehak-ro, Yuseong-gu, Daejeon, 34134, Republic of Korea
[i] Research Centre for Soil & Water Resources and Natural Disaster Prevention (SWAN), National Yunlin University of Science and Technology, Douliou, Yunlin, 64002, Taiwan
[j] Department of Safety, Health, and Environmental Engineering, National Yunlin University of Science and Technology, Douliou, Yunlin, 64002, Taiwan
[k] Department of Chemical Engineering, College of Engineering, King Saud University, P.O. Box - 800, Riyadh, 11421, Saudi Arabia
[l] Department of Nanotechnology Engineering, College of Engineering, Pukyong National University, Busan, 48513, Republic of Korea

ARTICLE INFO

Keywords:
Surfaces
Interfaces
Materials and nanomaterials
London surface energy
Lewis acid-base parameters
Bio-materials and pharmaceuticals

ABSTRACT

Inverse gas chromatography (IGC) has emerged as a highly sensitive, adaptable, and effective technology for material analysis. Through employing thermochemical approaches, IGC provides crucial insight into physico-chemical information of materials such as dispersive surface free energy, Gibbs surface energy components and Guttamann Lewis acid-base parameters. In this comprehensive review, we delve into the historical background, instrumentation, and diverse applications of IGC. Researchers and practitioners will find valuable information on the selection and description of numerous models used in IGC experiments. The applications of IGC span various domains, including polymers, medicines, minerals, surfactants, and nanomaterials. Furthermore, IGC facilitates the measurement of important parameters such as sorption enthalpy and entropy, surface energy components (dispersive and specific), co/adhesion work, glass transition temperature, surface heterogeneity, miscibility, solubility parameters, and specific surface area. These insights contribute to a deeper understanding of material behavior and aid in the design and optimization of advanced materials. Moreover, the integration of computer vision and image processing techniques with IGC has enhanced our understanding of materials intricate surface texture, roughness, and related properties. This convergence of IGC with computer vision and artificial intelligence (AI) presents exciting opportunities for future exploration of chemical materials, opening new avenues for research and discovery. This paper not only provides a comprehensive overview of IGC, its techniques, and applications but also highlights the synergistic potential of combining IGC with AI and computer vision. The informative content and insights presented here will benefit researchers, scientists, and professionals in the field of advanced materials, enabling them to leverage IGC and AI for innovative materials discovery and development.

* Corresponding author.
E-mail address: kimcw@pknu.ac.kr (C.W. Kim).

https://doi.org/10.1016/j.trac.2024.117655
Received 11 October 2023; Received in revised form 13 March 2024; Accepted 15 March 2024
Available online 16 March 2024

1. Introduction

Inverse gas chromatography (IGC) has evolved as a powerful technique for investigating the physicochemical properties of materials. Its origins can be traced back to the pioneering work of Martin and Synge, who utilized chromatography to determine partition coefficients of liquids [1]. Nevertheless, it was the contributions of researchers such as Wicke, Glueckaf, Cremer and Prior, and James and Phillips that demonstrated the potential of gas chromatography (GC) for physicochemical investigations, including the determination of adsorption isotherms [2]. In the early 1960s, A. V. Kiselev a prominent researcher in surface chemistry and chromatographic research, introduced the term "inverse gas chromatography" to describe the utilization of GC for studying solid surface properties [3,4]. Kiselev and his co-authors discussed the broad range of capabilities of GC in determining characteristics such as activity coefficients, entropies and heats of solution, molecular weight, vapor pressure, adsorption isotherms, surface free energies, diffusion coefficients, heat and adsorption entropies, internal diffusion activation energies, and hydrocarbons boiling points. During the 1960s, the orderly use of GC for computing the physicochemical parameters of solid surfaces gained significant attention [5–13].

Smidsrod and Guillet made significant contributions to the advancement of IGC by utilizing GC to study nonvolatile materials [14]. In IGC, nonvolatile materials are utilized as stationary phases, and their interactions with volatile solute probes are measured to obtain information about their physical and chemical states [15–18]. This approach offers a flexible, precise, and efficient means of measuring thermodynamic and physical properties of nonvolatile materials with respect to temperature range. Specifically, IGC offers valuable insights into solute-polymer interactions in highly concentrated polymer solutions, with numerous applications in industries alike inks, paints, solvent removal, surface coatings. The scope of IGC extends to the characterization of various nonvolatile materials, including polymers, biopolymers, conducting polymers, fibers, composites, hydrocarbons, paper, fillers, minerals, food products, drugs, and nanomaterials [19–30].

IGC has also been employed to investigate the interaction between different components in mixed stationary phases. For example, the Flory-Huggins interaction parameter can be determined via IGC for polymer blends and combinations of polymers with fibers or pigments [31]. Regarding its application in providing thermodynamic data, IGC serves as a valuable tool for studying a wide range of phenomena and properties. These include phase transitions, adsorption properties, surface energies and more [32,33]. The technique allows for the determination of various parameters, such as Kováts retention indices, molar Henry coefficients, partially molar free energy differences, solute weight fraction activity coefficients at infinite dilution, Hildebrand and Hansen solubility parameters [34]. It also enables the characterization of crystallinity in semi-crystalline polymers, evaluation of polymer surface roughness, analysis of phase separation in immiscible polymer blends, identification of surface regions in the stationary phase, measurement of melting temperature and glass transition temperature, determination of solid surface energy including dispersive and specific components, analysis of enthalpy and entropy of adsorption, and exploration of Lewis acid-base characteristics on solid surfaces [35]. These capabilities of IGC contribute to a comprehensive understanding of materials and their surface properties. The diverse range of data that can be obtained through IGC, coupled with the ongoing advancements in thermodynamic theory, positions this approach as indispensable for gaining insights into the behavior of materials in the field of materials science.

In addition to the progress made in IGC, the integration of artificial intelligence (AI) holds great promise for materials science and engineering. The advancements in AI and image analysis have significantly enhanced sensor-based data exploration in various image-based intelligent tasks, including object detection, classification, segmentation, action recognition, and pose estimation, using diverse sensor systems [36–42]. By combining IGC with AI image analysis techniques, machine learning, and data analysis algorithms, we can tap into new possibilities and gain deeper insights into the characterization and exploration of advanced materials. The convergence of IGC and AI opens up avenues for enhanced data processing, pattern recognition, and predictive modeling. Through AI-driven analysis, large datasets generated by IGC experiments can be efficiently processed, allowing for the extraction of hidden patterns and correlations. Machine learning algorithms can be trained to recognize complex surface interactions, classify materials based on their physicochemical properties, and predict material behaviors and performances. This integration holds great potential for accelerating materials discovery and development processes. AI algorithms can aid in the identification of optimal material compositions, surface modifications, and processing conditions. By leveraging the combined power of IGC and AI, researchers can streamline the search for materials with desired properties, leading to the design of novel materials with improved functionalities, enhanced performance, and tailored characteristics.

Furthermore, the integration of IGC and AI can extend beyond traditional materials science and engineering. It can pave the way for advancements in fields such as catalysis, energy storage, biomedical materials, environmental science, and beyond. The ability to rapidly characterize materials, understand their surface properties, and predict their behaviors through AI-driven analysis has far-reaching implications for an extensive scale of applications. Ultimately, the convergence of IGC and AI is poised to revolutionize the way we explore, understand, and engineer advanced materials. It offers the potential to accelerate the pace of material discovery, optimize material performance, and drive innovation across various industries. The integration of IGC and AI is expected to transform the landscape of materials science and engineering, enabling researchers to tackle complex challenges and unlock the full potential of advanced materials.

2. Fundamentals

2.1. Instrumentation and methods

IGC involves the transportation of the analyte through a column containing a liquid stationary phase using a gaseous mobile phase. The extent of contact between the analyte and the stationary phase, as well as its volatility, play crucial roles in determining its retention. To enhance volatility and reduce retention times, columns are typically maintained at elevated temperatures. The analysis of peaks and measurement of retention times were performed using the dual column GC-5890 HEWLETT PACKARD SERIES II (HP Ltd. Republic of Korea) software, which was connected to a personal computer. The GC system is equipped with packed columns, an injector, and a flame ionization detector (FID). A liquid crystal display (LCD) processor is incorporated into the apparatus to regulate the temperatures of the oven, injector, and detector.

Fig. 1 presents a schematic illustration of the GC system and Fig. 2 shows FID, a mass flow sensitive detector that requires three gases for operation. FID utilizes hydrogen and oxygen as fuel gases, along with nitrogen as the carrier gas, to create a flame. In the absence of sample molecules, the flame is deficient in charged particles. By applying 230 V between the flame and the collector electrode, the resulting residual current falls within the range of 10–12 A. This small current serves as the baseline signal, which is then amplified. When an organic solute molecule is eluted at the edge of the hydrogen flame, it produces CH, CH_2 and CH_3 radicals. These radicals interact with the excited molecules in the flame, generating positively charged ions and electrons. As a result, the current between the flame and the collector electrode increases, allowing for detection of the analytes relative to the baseline current. Analytes containing more CH- groups elicit a stronger detector response, leading to larger peak areas. Prior to entering the gas chromatograph, the three gases like nitrogen, hydrogen, and oxygen, pass through Hp Gas

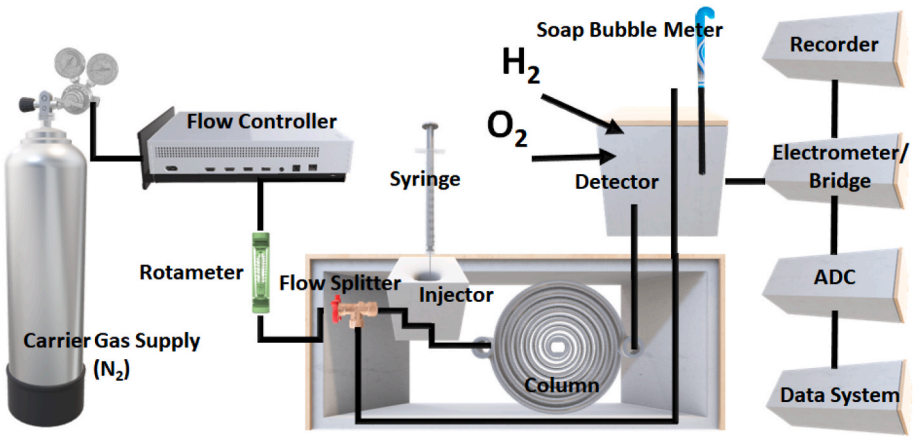

Fig. 1. Schematic representation of typical Inverse Gas Chromatography (IGC) analyzer.

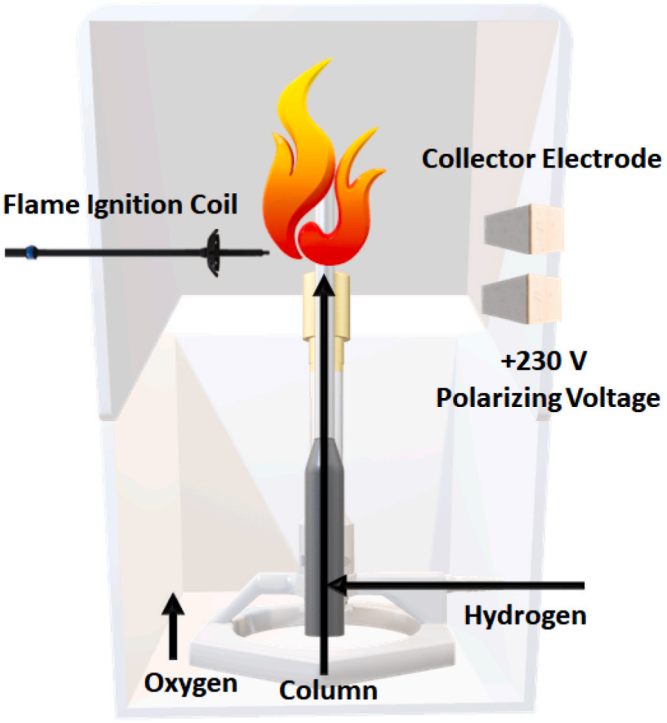

Fig. 2. A schematic illustration of flame ionization detector (FID).

purifiers to remove impurities such as oil, moisture, and other foreign substances. Molecular sieve is used to prevent particulates from entering the flow systems, and a frit is placed near the output as an additional measure.

To detect gas line leaks, a soap solution was applied to the suspected joints, and any leaks were identified by tightening the corresponding nut. The flow of the carrier gas at room temperature was determined using a soap film flow meter. The regulator was set to allow a carrier gas flow of approximately 30 mL/min through the column at the column temperature. The regulators for oxygen and hydrogen were adjusted to maintain a pressure of 0.75 kg/cm^2 for both gases. Initially, only hydrogen was turned on to ignite the flame, while oxygen and the carrier gas were kept off. The oxygen and carrier gas were opened after confirming the flame was lit by observing the FID exit.

Flame ionization detectors are commonly employed in GC due to several advantages. Mainly cost of flame ionization detectors are generally inexpensive to purchase and run. Low maintenance requirements. Other than cleaning or replacing the FID jet, these detectors require little attention. Rugged design FIDs are relatively resistant to misuse. FIDs have a linear response range of 107 g/s and can detect organic substances at low (10–13 g/s) to high quantities. The FID's destructive nature prevents it from being directly coupled to other GC detectors. However, an FID can still be used in conjunction with another detector if a portion of the carrier gas stream is shared between the two detectors. The presence of a condensation coating on the glass indicated a functioning flame. Precise control of hydrogen and oxygen was necessary to maintain a consistent flame and a stable baseline without noise. The oven, equipped with a Nichrome wire heating element and a platinum resistance thermometer, maintained a constant temperature for the column. A fan inside the oven ensured temperature uniformity, with accuracy up to ±10 °C. Separate heating systems were used for the injector and detectors, controlled by proportional solid-state controllers. Once thermal equilibrium was reached, the neon lights began to flicker, and a trigger pulse isolation transformer isolated the sensing circuit from the mains. Temperature feedback was provided by the platinum resistance thermometer, and an integrated circuit executed the logic function to regulate the power of the Nichrome heater using connected Triacs.

2.2. Theory of surface measurements by IGC

2.2.1. Net retention volumes

IGC theory and applications are covered in detail elsewhere [2,3]. the chemical potential of solute 'i' dispersing connecting the liquid phase (L) and the mobile phase (M) in the chromatographic column at constant temperature and constant pressure.

$$\mu_i^L = \mu_i^M \tag{1}$$

$$\text{or } \mu_L^0 + RT\ ln\ C_L = \mu_M^0 + RT\ ln\ C_M \tag{2}$$

$$ln\frac{C_L}{C_M} = \frac{\Delta\mu^0}{RT} = \frac{\left(\mu_M^0 - \mu_L^0\right)}{RT} = ln\ K \tag{3}$$

where C_L and C_M are solute i concentrations in phases L and M, respectively, μ is the standard chemical potential difference, and K is the solute partition coefficient in Eqs. (1)–(3). The linear rate of travel is identical to the average carrier velocity multiplied by the fraction of time the solute passes in the mobile phase.

$$\text{Rate of travel} = \overline{u}\left(\frac{C_M V_M}{C_M V_M + C_L V_L}\right) = \overline{u}\left(1 + K\frac{V_L}{V_M}\right)^{-1} \tag{4}$$

V_M and V_L are the volumes of the mobile and stationary phases. Alternatively, the solute rate of travel can be calculated as

$$\text{Rate of travel} = \frac{column length, L}{retention time, t_R} \tag{5}$$

2.2.1.1. Eqs. (4) and (5) Gives

$$t_R = \frac{L}{\overline{u}}\left(1 + K\frac{V_L}{V_M}\right) \tag{6}$$

The quantity $L/\overline{u}$ is the retention time for non-interacting solute (Ne or CH_4) represented as t_M in Eqs. (6) and (7).

$$t_R = t_M\left(1 + K\frac{V_L}{V_M}\right) \tag{7}$$

The determined flow rate, F, is to be adjusted to the states be happening in the column using Eq. (8).

$$F_C = F\left(\frac{T}{T_r}\right)\left(\frac{P_o - P_w}{P_o}\right) \tag{8}$$

where T is column temperature, T_r is room temperature, P_o and P_w are the outlet pressure and water vapor pressure at T_r. Since $t_R F_c = V_R^{'}$ and $t_M F_c = V_M^{'}$, Eq. (7) can be composed as

$$V_R^{'} = V_M^{'}\left(1 + K\frac{V_L}{V_M}\right) \tag{9}$$

The correction factor for the pressure gradient across the column, according to Martin and James [43], is given by

$$\mathrm{J} = \frac{3}{2}\left[\frac{(P_i/P_0)^2 - 1}{(P_i/P_0)^3 - 1}\right] \tag{10}$$

where P_i and P_0 are inlet and outlet pressures. The fully corrected form, Eq. (9) is

$$JV_R^{'} = JV_M^{'}\left(1 + K\frac{V_L}{V_M}\right) \tag{11}$$

$$V_R = V_M\left(1 + K\frac{V_L}{V_M}\right) = V_M + KV_L \tag{12}$$

$$V_R - V_M = V_N = KV_L \tag{13}$$

V_N is the net retention volume.

2.3. Surface energy and acid-base parameters of solid surfaces by IGC

2.3.1. Thermodynamic consideration of solid surfaces by IGC

The net retention volume, V_N in inverse gas-liquid chromatography can be broken down into two terms: one related to bulk absorption and the other to surface adsorption [44,45]. Consequently, it is possible to present

$$V_N = K_a V + K_s A \tag{14}$$

where V and A are the volume and surface area of the adsorbate, respectively, and K_a and K_s are the partition coefficients for the bulk absorption and surface adsorption, respectively. Eq. (14) for inverse gas solid chromatography can be reduced to

$$V_N = K_S A \tag{15}$$

The partition function, K_S accounts for the probe excess concentration on the surface, τ, and its concentration in the gas phase, C.

$$K_S = \frac{d\tau}{dc} \tag{16}$$

Under infinite dilution of the probe Henry's law is obeyed and therefore

$$\left(\frac{d\tau}{dc}\right)_{\tau\to 0} = \frac{\tau}{c} \tag{17}$$

Additionally, under ideal circumstances, the probe concentration in the gas phase can be expressed by

$$C = \frac{P}{RT} \tag{18}$$

where P is partial pressure of the probe and R is gas constant. Therefore, form Eqs. (17) and (18) can be derive as [46,47]

$$K_S = \tau\frac{RT}{P} \tag{19}$$

Following Gibbs equation τ is concerned to pressure on the surface

$$\tau = \frac{1}{RT}P\left(\frac{d\pi}{dP}\right) \tag{20}$$

where π is the pressure of the probe on the surface and $\left(\frac{d\pi}{dP}\right)$ measures how much the probe reduces the stationary phase's surface free energy. In the case of infinite dilution,

$$\frac{d\pi}{dP} \to \frac{\pi}{P} \tag{21}$$

Therefore, from Eqs. (15) and (21)

$$K_S = \frac{\pi}{P} = \frac{V_N}{A} \tag{22}$$

According to Santos [47], the surface free energy changes when 1 mol of probe molecules are adsorbed from a reference gas phase at a pressure P_g^S of to a reference adsorption phase at a pressure of P_s^S.

$$\Delta G_a = -RT\,ln\left(\frac{P_s^S}{P_g^S}\right) \tag{23}$$

Since, from Eq. (22), $P_g^S = \frac{\pi A}{V_N}$, thus

$$\Delta G_a = -RT\,ln\left(\frac{V_N P_s^S}{\pi A}\right) \tag{24}$$

For a particular stationary phase, A is fixed, P_s^S and π are constants. According to $\pi = 3.38 \times 10^{-4}\ Nm^{-1}$ and $P_s^S = 101.3\ kPa$. A is specific surface area of adsorbent and hence Eq. (24) can be written as [44,45],

$$\Delta G_a = -RTlnV_N + K \tag{25}$$

K is a constant which involves all the constants shown in Eq. (25).

2.3.2. Dispersive surface free energy of solid surfaces

IGC employs various approaches in the determination of the dispersive component of surface free energy of solid surfaces. Fowke's method [48–51] is based on his definitions of work of adhesion W_a between two non-polar species. Thus

$$W_a = 2\sqrt{\gamma_S^d \gamma_l^d} \tag{26}$$

where γ_S^d and γ_l^d dispersive component of solid and liquid surface tensions, respectively. The molar free energy of adsorption, according to Fowke's, can be defined as

$$-\Delta G_a = \mathcal{N}aW_a + K^{'} \tag{27}$$

where N is Avogadro's constant and a is the adsorbed solute's molecular surface area. Schultz et al. [52] connected the net retention volume to the molar free energy of adsorption in Eqs. (25)–(27), and the expression is given as

$$RTlnV_N = 2\mathcal{N}a\sqrt{\gamma_S^d \gamma_l^d} + K^{''} \tag{28}$$

From Eq. (28), a plot of $RTlnV_N$ versus $a(\gamma_l^d)^{0.5}$ for n-alkanes will yield a slope of $2\rightleftarrows N(\gamma_s^d)^{0.5}$ and an intercept of K'. The literature contains $a(\gamma_l^d)^{0.5}$ values for apolar and polar solute probes [49–51]. The surface free energy diagram shown in Fig. 3. The slope values can be used to calculate the dispersive component of the surface free energy γ_s^d of a solid surface. Because of the following reasons, the γ_s^d values obtained by this procedure may not always be trustworthy. Because of surface forces, the molecular regions may be deformed [51]. In the interface, non-spherical molecules such as n-alkanes may lie flat or head to tail. Furthermore, the effect of temperature on the molecular area is not considered. There are several ways for estimating the molecular surface area of probes, each of which yields a different value [53].

Dorris and Gray et al. [54], suggested another approach for calculating the dispersive component of the surface free energy γ_s^d using the Eq. below.

$$\gamma_s^d = \frac{\left[RT\ ln\left(\frac{V_N^{C_{n+1}H_{2n+4}}}{V_N^{C_nH_{2n+2}}}\right)\right]^2}{4N^2.(a_{CH_2})^2\gamma_{CH_2}} \quad (29)$$

where γ_{CH_2} is the surface area of a methylene, $-CH_2-$ group. The quantity of this parameter is presumed to be identical to 6 Å^2, N is Avogadro's number, γ_{CH_2} is calculated according to the following Eq. (30).

$$\gamma_{CH_2} = 35.6 - 0.058t \quad (30)$$

where t is the temperature in degrees Celsius. Considering the determination of a_{CH_2}, some papers discuss that the key challenge in this strategy is estimating a_{CH_2} and γ_{CH_2} [55]. According to Belgacem and Gandini [45], using Eq. (30) will get the most accurate γ_{CH_2} readings. The fluctuation of γ_s^d with the ratio of the net retention volume of two successive homologous n-alkanes is frequently considerable. Variations of the London dispersive surface free energy shown in Fig. 4. As a result, it is advised that the average of three pairs of n-alkanes to be used. The values of γ_s^d calculated using Fowke's and Dorris - Gray approaches were found to be similar by Voelkel et al. [56], and Shi et al., [57].

The free energy of adsorption of each probe is displayed as a function of logarithm of the probe vapor pressure at the column temperature in the Papirer and Saint-Flour approach [46,49,58]. A straight line with a negative slope is produced for n-alkanes. The slope can be applied to describe the surface's capability to endure dispersive interactions. This method rejects the errors in Fowke's method's estimation of 'a' of the probe. At different temperatures, other γ_l^d values are also unavailable. Another strategy, considerably less commonly used, is that of Sawyer and Brookman, which makes use of the probe's boiling point [59]. Donnet et al. developed another way for high dispersive energy surfaces based on molar deformation polarization of the probing molecule [60]. The technique of Brendlé and Papirer is based on the usage of the probe's topological index [61].

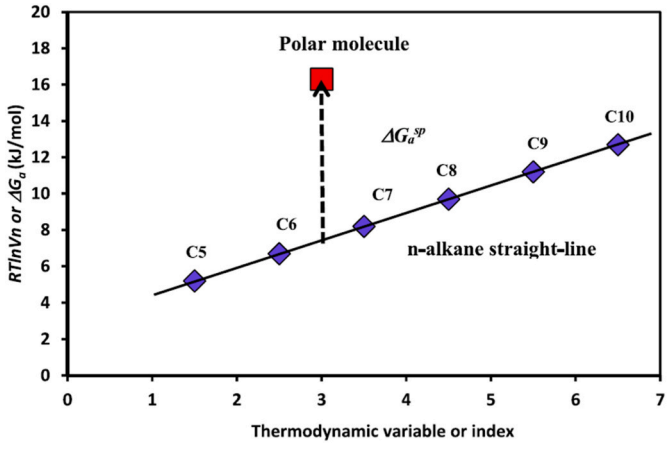

Fig. 3. Variations of $RTlnV_N$ of n-alkanes and polar probes as a function of a thermodynamic variable or index of a solid at fixed temperature.

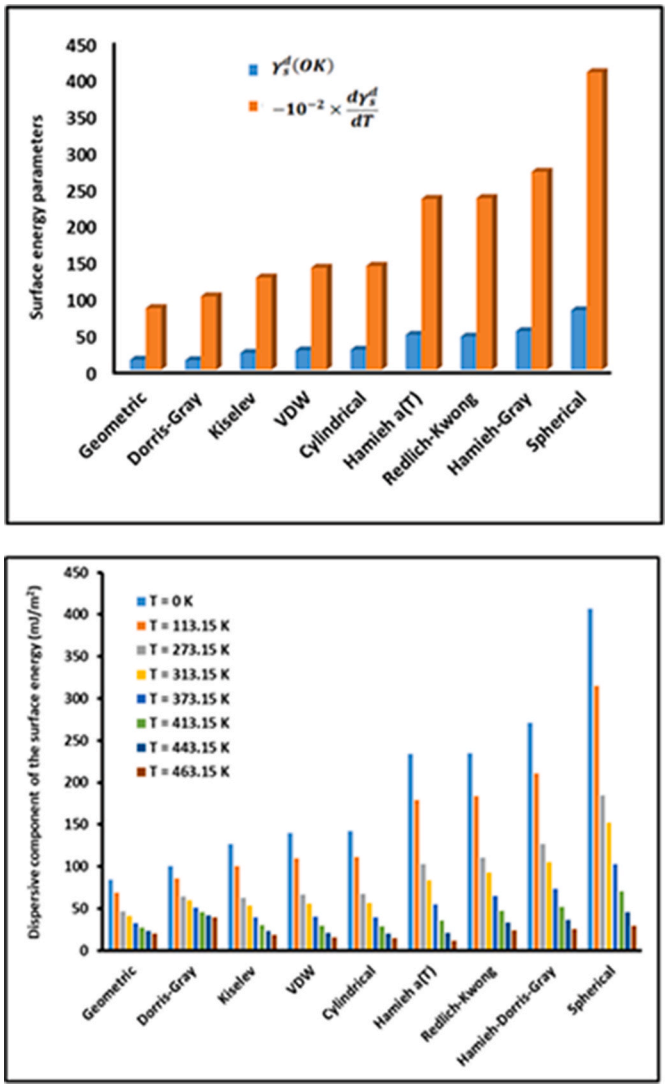

Fig. 4. Variations of the London dispersive surface free energy (γ_s^d) depending on the chosen model or IGC method.

3. Lewis acid-base interaction capability of a solid surface

A Lewis acid is an ion or molecule that admits an electron pair from the probe solute. A Lewis base is a molecule or ion that can donate an electron pair to a probe solute, causing coordination bonds to form [62]. In the case of polar solutes, Lewis acid-base interaction arises, and there is a corresponding particular component of adsorption free energy. As a result, the overall free energy of adsorption includes two terms: one due to the exact component and one related to the dispersive component. Thus

$$\Delta G_a = \Delta G_a^d + \Delta G_a^S \quad (31)$$

Here, ΔG_a^d is the term that characterizes the dispersive Lifschitz - van Der Waals involvement to the total free energy of adsorption, ΔG_a the probe used for the determination ΔG_a^d of are n-alkanes. ΔG_a^S corresponds to the Lewis acid - base (specific) interaction contribution to ΔG_a. Commonly

used polar probes for determination of ΔG_a^S are including trichloro methane (TCM), diethyl ether (DE), Acetone (AC), dichloromethane (DCM), ethyl acetate (EA) and tetrahydrofuran (THF).

The determination of ΔG_a^S can be brought out in detail using Fowke's plot drawn between $RTlnV_N$ versus $a(\gamma_l^d)^{0.5}$. Fowke's plots for a homologous series of n-alkanes yields and shows a straight line, which supports a linear regression relating $a(\gamma_l^d)^{0.5}$ and $RTlnV_N$. From Eqs. (25) and (31) the specific component of the free energy of adsorption ΔG_a^S is given by

$$-\Delta G_a^S = RT\ ln\left(\frac{V_N}{V_{N,ref}^d}\right) \tag{32}$$

where V_N is the retention volume of the polar probe with a precise $a(\gamma_l^d)^{0.5}$ value and $V_{N,ref}^d$ is the retention volume that is gained from the n-alkane reference line at the identical value of $a(\gamma_l^d)^{0.5}$. Usually, the polar solutes fall above the n-alkane reference line in the Fowke's plot indicating that $-\Delta G_a^S$ values are beyond negative for polar probes compared to the n-alkane reference line. If mono polar probes are used in the characterization of adsorbent, the interaction with a Lewis basic probe is a compute of the Lewis acidity of the surface. On the contrary, the Lewis acidic probe will go through given interactions with basic sites on the adsorbent.

A plot of $\Delta G_a^S/T$ versus $1/T$ for polar probes bears the certain component of enthalpy of adsorption, ΔH_a^S and the certain component of entropy adsorption, ΔS_a^S. The variations of $\Delta G_a^S/T$ are shown in Fig. 5. Both the Lewis acidity and the Lewis basicity of a material provide to the value of ΔH_a^S. The methodology of Gutmann admits for the quantification of the Lewis acidity and Lewis's basicity of a material from ΔH_a^S values [63]. The Lewis acidity parameter, K_a, and Lewis basicity parameter, K_b, is calculated using the following relation.

$$-\Delta H_a^S = K_a \times DN + K_b \times AN^* \tag{33}$$

where DN and AN^* are Guttmann's donor [64] and Riddle and Fowke's [65] altered acceptor numbers correspondingly. Plotting $-\Delta H_a^S/\ AN^*$ against DN/AN^* gives K_a as the slope and K_b as the intercept. The Variations of $\left(\frac{-\Delta H_a^{sp}}{AN}\right)$ as a function of $\left(\frac{DN}{AN}\right)$ of different polar molecules shown in Fig. 6. The parameters K_a and K_b communicate the capability of the investigated material to act as electron acceptor (acidic) and electron donor (basic) respectively. Fekete et al. observed the consistency of numerous attempts of estimation of K_a and K_b [66]. Grajek studied the errors in the parameters [67]. γ_s^d, K_a and K_b parameters are useful for alteration of solid surfaces [68]. The awareness of γ_s^d is crucial

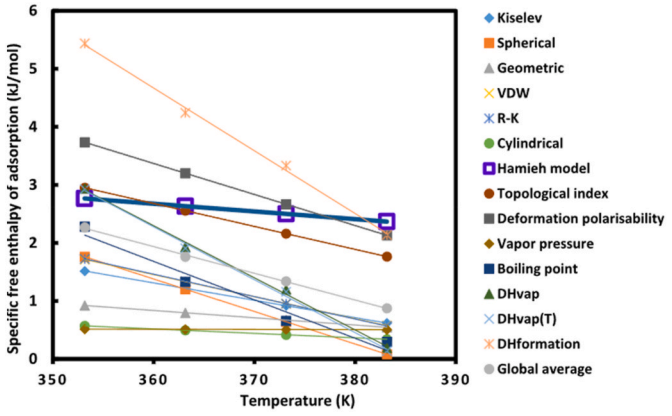

Fig. 5. Variations of $-\Delta G_a^{sp}$ (T) as a function of the temperature by using the various chromatographic models or methods.

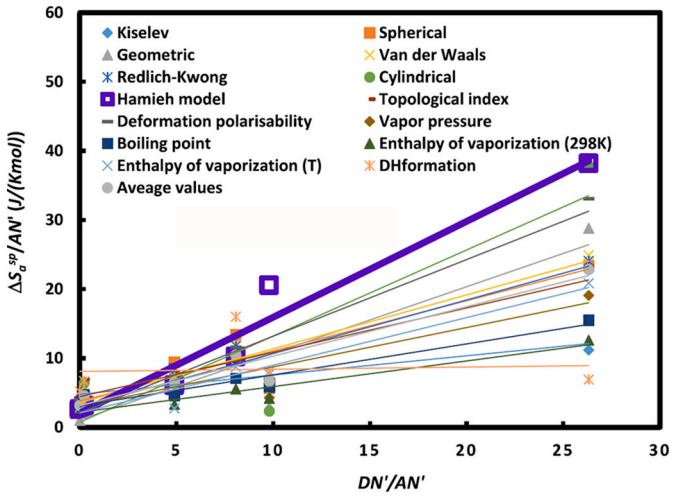

Fig. 6. Variations of $\left(\frac{-\Delta S_a^{sp}}{AN}\right)$ as a function of $\left(\frac{DN}{AN}\right)$ of different polar molecules in polymer surface for different molecular models and IGC methods.

to emulsion and suspension production [69] and in the assessment of adhesion [70].

Hamieh et al. proved in several studies that the Gutmann method cannot be applied because the linearity of the previous relation is not satisfied [71–73]. They proposed a new equation considering the coupled amphoteric character of some solid substrates by introducing a third parameter K [71–73]. The new proposed expression was:

$$-\Delta H_a^S = K_a \times DN + K_b \times AN - K \times AN \times DN \tag{34}$$

Or

$$\left(\frac{-\Delta H^{Sp}}{AN}\right) = K_A\left(\frac{DN}{AN}\right) + K_D - K\ DN \tag{35}$$

Eq. (35) can be written as:

$$X_1 = K_D + K_A X_2 - KX_3 \tag{36}$$

Where

$$X_1 = -\frac{\Delta H^{sp}}{AN}, X_2 = \frac{DN}{AN}, X_3 = DN \text{ and } K = K\ (K_A, KD) \tag{37}$$

Note that $X1$, $X2$ and $X3$ are identified for every polar molecule, whereas K_D, K_A and K are unfamiliar.

Hamieh et al. gave the unique solution of the linear organization of three equations with three unknown variables: K_D, K_A and K by showing that the matrix indicating this linear application is a symmetrical one for polar solvent number $N \geq 3$.

A review of the literature indicated that Voelkel et al. [74], studied the dispersive surface energy and acid-base characteristics of various materials, and Hancock et al. [75], reviewed pharmaceutical materials. The literature on some recent work is offered here. Ballard et al. [76], reported on the surface properties of micro granular and micro fibrous cellulose, and Wang et al. [77], investigated the acid-base properties of porous cellulose beads. Mills et al. [78], reported the dispersive surface free energy of high-cellulosic fiber. IGC was used to evaluate the surface properties of microcrystalline cellulose [79,80] and cellulosic multipurpose office paper [81]. Some materials' surface properties have been reported, including milled graphite, sucrose, toner particles, active carbon, carbon nanotubes, cement components, alumina, chitin and sepiolite [82–91]. IGC measurements of cellulose esters' surface characteristics and contact angle measurements of cellulose esters have been reported [92]. Researchers investigated the dispersive surface energy of cellulose Nano whiskers and nanocomposites [93]. Surface thermodynamic characteristics of conducting polymers, poly aniline, and their

mixtures have been studied [94,95].

3.1. Critics to the different chromatographic methods

Among all previous methods, it seems that the most used method for the determination of the specific interactions between a solid surface and model organic molecules was that of Saint-Flour and Papirer [148,149] based on the vapor pressure of the probes that varies with temperature. The serious difficulty with this method is to determine with good accuracy the acid-base constants of certain mineral, metal oxides, zeolites and/or nanomaterials. The theoretical basis of the representation $RTlnV_n = f(logP_0)$ cannot be scientifically justified, even if one obtained a perfect linearity. Hamieh proved the linearity of ΔG_a^0 or $RTlnV_n$ of adsorbed n-alkanes as a function of any physical, chemical or thermodynamic surface parameters was always satisfied with an excellent linear regression coefficient [96]. The same observation was shown with the representation of $RTlnV_n$ as a function of boiling point (B·P.), the standard enthalpy of vaporization ΔH_{vap}^0 or the topological index χ_T of n-alkanes where negative values of acid or base constants of solids were obtained in several cases leading to conclude to the non-validity of such methods.

On the methods well-theoretically founded was that based on Fowkes relation and using the variations of $RTlnV_n$ as a function of $2\mathcal{N}a\sqrt{\gamma_l^d}$. However, the serious problem of this method was related to the estimation of the dispersive surface energy component γ_s^d of a solid, with the help of the surface areas of n-alkanes. This surface area is not known with accuracy. Hamieh first proposed the use of the following models giving the molecular areas of n-alkanes: the geometrical model, cylindrical molecular model, liquid density model, BET method, Kiselev results and the model using the two-dimensional van der Waals (VDW) constant b that depends on the critical temperature and pressure of the liquid were measured. Another equation also used was the Redlich-Kwong (R–K) equation transposed from three-dimensional space to two-dimensional space to calculate the areas of organic molecules. Hamieh concluded that the dispersive surface energy γ_s^d of solid materials varies substantially on the selected molecular models of the surface area of n-alkanes and on the temperature [71,96,97].

The recent results reported by Hamieh group gave the respective expressions of the dependence of the surface areas $a(n,T)$ of n-alkanes and $a_X(T)$ of polar molecules against the temperature [98,99].

For n-alkanes, he obtained:

$$a(n,T) = \frac{69.939\,n + 313.228}{(563.02 - T)^{1/2}} \tag{38}$$

For polar solvents, Hamieh gave relation.

$$a_X(T) = a_{Xmin.} \times \frac{(T_{Max.1} - T)}{(563.02 - T)^{1/2}\left(T_{Max.(X)} - T\right)^{1/2}} \tag{39}$$

Where n is the carbon atom number of n-alkane, and $T_{Max.1}$ and $T_{Max.(X)}$ are two new intrinsic surface parameters of polar molecules.

Thus, Hamieh resolved that the Fowke's method proposed by Schultz et al. cannot be utilized to establish the dispersive surface energy nor to assess the specific interactions. The results attained by this approach are imprecise. Consequently, the values of ΔG_a^{sp} and γ_s^d acquired by numerous researchers and the conclusions ensuing from these incorrect values have to be considered as imprecise.

Another interesting chromatographic method was proposed by Donnet et al. considering the deformation polarizability α_0 for the determination of London dispersive forces and specific interactions between adsorbate and adsorbent [60]. They plotted the variation of $RTlnVn$ as a function of $(h\nu_L)^{1/2}\,\alpha_{0,l}$ for all used probes, where ν_L is the electronic frequency of the probe and h the Planck's constant. Unfortunately, this method cannot be used without committing large errors in the determination of the surface parameters of solids. Indeed, even if this method was based on solid theoretical concept; however, the it neglected the harmonic mean of the ionization energies of the solid and the adsorbed organic molecules as was shown by Hamieh in a recent study who proposed the full London equation to determine the dispersion interaction energy between the solid and the probes [100].

3.2. Computer vision and image processing (CVIP) pipelines for SEM analysis

The powerful image analysis in 2D domain is one of the fundamental means of retrieving and analyzing data and there are various tools to achieve the precision in image analysis. The image analysis and interpretation of the image data spans the application scenarios from basic image processing to AI applied on various fields such as agriculture, robotics, autonomous vehicles and computational chemistry [101–106]. The IGC exploits the thermodynamic surface characterization of the compound while the CVIP tools are employed to reveal the intricate visual properties such as surface morphology, 3D roughness, directionality, and particle area distribution. The significance of these visual traits and intricate details can be viewed alongside the IGC findings to consider a certain compound for research purposes. The customized pipeline for revealing the visual properties can be applied on any compound of interest that is considered for the IGC examination. The example CVIP customized algorithms and relevant workflows are illustrated in Fig. 7.

3.2.1. Intricate visual traits

The compound considered for the IGC experiments can be investigated for its intricate visual traits using the CVIP tools. In particular, the SEM image is initially visualized in 3-color channel RGB is converted to the gray scale for further inspection. The observable specimen is then considered with a specific region-of-interest (ROI) and extracted from the original specimen; this supports the further 3D examination of the compound. The computer vision image processing algorithms such as the anisotropic diffusion [107] and total variation ROF (Rudin, Osher, Fatemi) denoising [108] were applied on to the extracted ROI to avail the noise removal induced by the SEM instrument without removing the intricate edge information.

3.2.2. Surface roughness

The extracted specimen ROI is utilized for the surface morphology in determining the lumps and valleys in the compound surface. The computer vision methods such as Fast Fourier Transform (FFT) is applied on the specimen which transform the image pixels of the compound to the frequency domain to estimate the noise elements in the high frequency components [109]. The pipeline is then transformed back to the pixel domain using inverse FFT to reduce the noise. The resultant specimen often contains several intensity values with improper distribution of the pixel values.

3.2.3. Particle distribution, porosity and directionality

The particle distribution gives the crucial information on the compound's surface distribution and conductivity in general. In addition to the particle distribution, the porosity and directionality of the specimen can be determined using the computer vision algorithms and Image J tool [110]. The extracted specimen is used to calculate the threshold using image processing algorithms such as binary and otsu thresholding [111]. The thresholding reveals the foreground objects (particles) and their distribution in the specimen which can be statistically analyzed using several metrics and relevant values of mean, standard deviation can be estimated.

Additionally, the cross-sectional surface area of the particles and selected ROI of the specimen can be estimated using the statistical analysis. The porosity and pore size estimation can also be determined using the computer vision algorithms [112] which provides the insight

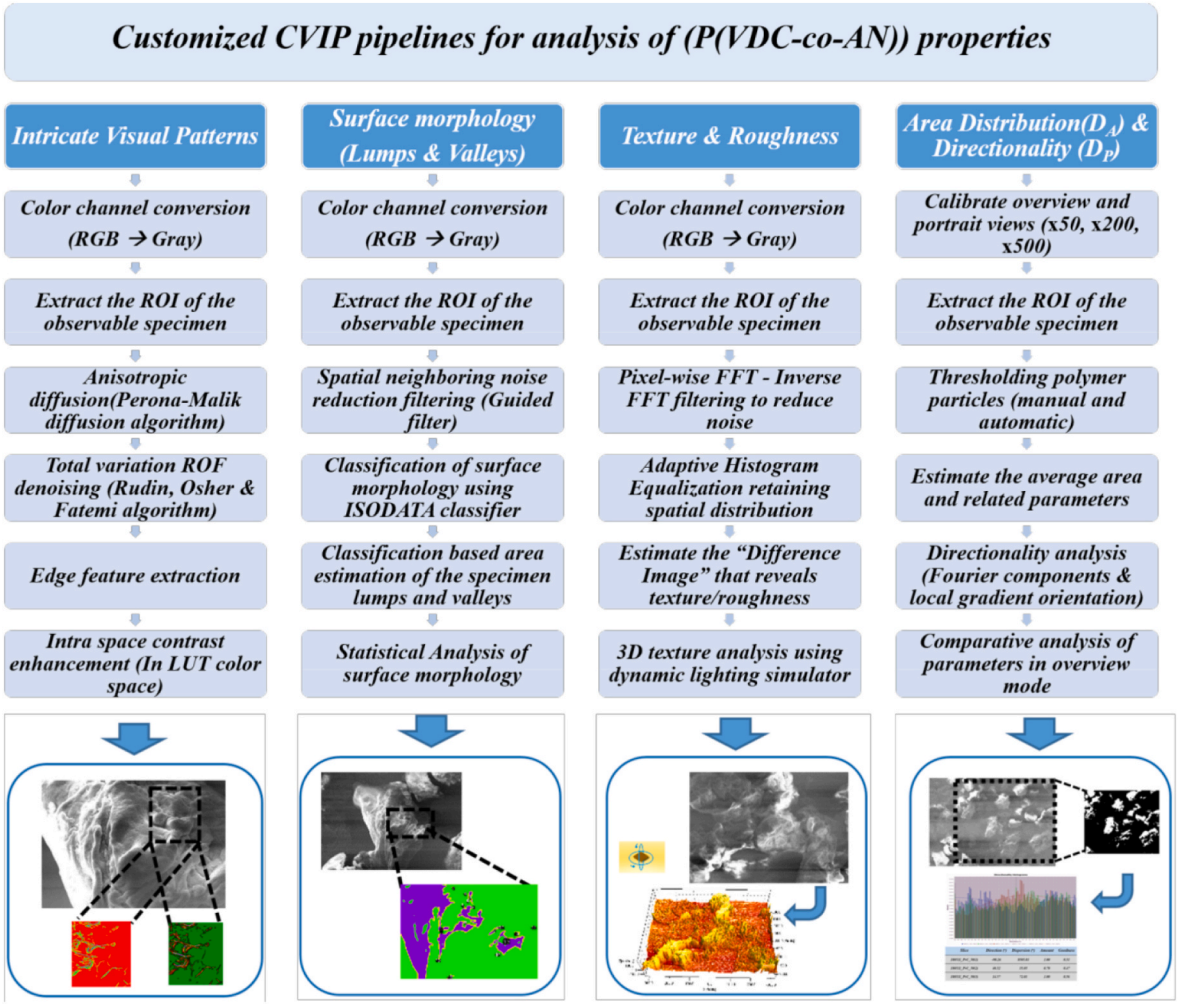

Fig. 7. Customized CVIP pipelines for analysis of polymer properties.

on how the compound particles are distributed on the surface. Additionally, the directionality of the individual particles can be obtained using the directionality analysis of the specimen.

3.3. Vision intelligence scenarios for IGC

The integration of vision intelligence scenarios such as automated image processing, real-time monitoring and improved accuracy and precision can be categorized as the computer vision-based scenarios that are applicable in the IGC domain. Similarly, AI-driven machine learning algorithms, predictive modeling and optimization of experimental parameters are categorized as the AI-based scenarios that are applicable in the IGC domain.

3.3.1. Computer vision-based IGC scenarios

Computer vision techniques are essential for automating the processing of chromatograms acquired from IGC experiments. By employing image segmentation, feature extraction, and pattern recognition algorithms, the time-consuming task of manual analysis is substituted with efficient and precise automated procedures. The very early studies conducted by Castellano, M. et al. [113] explores further utilizing both inverse gas chromatography (IGC) and image analysis assisted transmission electron microscopy (TEM/AIA) to examine filler dispersion and morphology, in addition to the commonly studied surface characteristics and thermodynamics. This integrated methodology provides essential understanding of the relationship between filler properties and the interactions between polymers and fillers, facilitating the development of optimized tire tread formulations. The general scenario of the stages involved in the automated image processing for IGC is illustrated in Fig. 8. The immediate monitoring of chromatographic peaks, enabling fast data collection and analysis can also be achieved using computer vision techniques. Through the continual monitoring of alterations in the forms and strengths of peaks, scientists may promptly detect and examine developing trends, resulting in better-informed decisions. Kochmann et al. reported the image based peak analysis and detection approaches for electrophoresis data which can be opted for the IGC data with an adhoc approach [114].

3.3.2. AI-based IGC scenarios

AI-powered machine learning methods, such as neural networks and support vector machines, are utilized to analyze intricate IGC datasets. These algorithms possess the ability to detect nuanced connections and patterns within the data, hence offering more profound insights into the characteristics and behavior of materials. Through utilization of AI approaches to create models that can estimate material qualities from IGC data. These algorithms can effectively predict material properties, thus enhancing the efficiency of product creation and optimization. AI optimization algorithms are used to improve the efficiency and effectiveness of IGC studies. These factors include temperature and flow rate. By employing iterative learning and adaptation, these algorithms determine the most favorable conditions for attaining desired analytical results, hence maximizing productivity and the efficient use of resources. A few studies such as Martakidis et al. used the microcontroller to log the temperature and reversed flow for the IGC measurements and optimized

Scenario 1 Automated Image Processing in IGC

Start
Image Acquisition: Obtain chromatograms from IGC experiments.
Preprocessing:
    Apply filters to enhance image quality.
    Remove noise and artifacts.
Image Segmentation:
    Divide the chromatogram image into individual peaks.
    Use techniques like thresholding or clustering to separate peaks from background.
Feature Extraction:
    Identify key features of each peak, such as area, height, and width.
    Extract numerical descriptors to characterize the peaks.
Pattern Recognition:
    Employ pattern recognition algorithms to classify peaks based on their shapes and characteristics.
    Determine peak types (e.g., Gaussian, exponential) and distinguish between different compounds.
Automated Analysis:
    Analyze the segmented peaks to calculate relevant parameters, such as retention time and peak area.
    Generate quantitative data for each peak.
End

Fig. 8. Algorithm explaining automated Image Processing In IGC.

the whole process [115]. A general pipeline of optimization stages was illustrated in Fig. 9, which is approach-specific, the objective function and experimental parameters are defined by the researchers.

4. Applications

IGC has emerged as a convenient and accurate approach for measuring physicochemical parameters, leading to its extensive application in studying a wide range of materials. One of the key advantages of IGC is its ability to characterize the physicochemical properties of non-volatile substances in various forms and morphologies. It enables the characterization of both bulk and surface properties, including surface free energy components, surface coverage, phase transitions, diffusion coefficients, crystallinity, and surface characteristics such as area, free energy, acidity-basicity, and porosity. These precise surface characterization capabilities make IGC a valuable tool for predicting the behavior of a material's surface when it interacts with other substances or for identifying surface property changes resulting from production processes.

For instance, IGC has been successfully used to predict the mass and surface property changes of medicinal molecules due to milling, which is of great importance in the pharmaceutical industry. In addition, IGC can provide insights into polymerization processes by determining miscibility, solution parameters, and Flory-Huggins interaction parameters. Researchers, such as Voelkel et al. [116], have discussed the application of IGC in quantifying the physicochemical characteristics of diverse materials [117]. IGC is often referred to as a physico-chemical characterization technique as it allows for simultaneous measurement of both physical and chemical properties of materials. In a recent application, the structural and chemical properties of carbon nanotubes were examined using two sets of probes with different chemical specificity, known as "structural probes" and "chemical probes" [118]. This review covers the use of IGC in analyzing the surface characteristics of a wide range of substances, ranging from natural minerals to pharmaceutical products, highlighting the diverse applications that can benefit from IGC.

4.1. Polymers

Polymers have gained significant attention in IGC due to their

Scenario 2 Optimization of Experimental Parameters in IGC

Start
Experimental Design:
    Define the experimental objectives and constraints.
    Specify the range of parameters to be optimized, such as temperature, flow rate, or column length.
Data Collection:
    Conduct IGC experiments using various parameter settings.
    Collect data on peak characteristics and material properties.
Data Preprocessing:
    Clean and preprocess the experimental data.
    Standardize data formats and remove outliers.
Model Training:
    Train AI algorithms, such as genetic algorithms or reinforcement learning models, to optimize experimental parameters.
    Define the objective function to be maximized or minimized.
Optimization:
    Utilize the trained AI algorithms to search for optimal experimental parameters.
    Iteratively adjust parameter settings based on algorithm feedback and performance metrics.
Validation:
    Validate the optimized parameter settings using experimental data or simulation techniques.
    Ensure that the optimized parameters result in improved analytical outcomes.
Implementation:
    Implement the optimized experimental parameters in IGC experiments.
    Monitor performance and adjust parameters as necessary.
End

Fig. 9. Algorithm explaining optimization of Experimental Parameters in IGC.

adhesive nature. IGC can effectively assess the porosity of synthetic polymers, biological polymers, copolymers, and polymer blends across a wide temperature range. Surface characterization of polymers below the glass transition temperature (T_g) enables the monitoring of surface changes resulting from chemical modifications. Additionally, IGC can calculate dimensional Hansen solubility parameters and Flory-Huggins interactions, providing insights into material interactions, composite component miscibility, and polymer solubility in liquids. However, it is important to note that this technique may not be applicable in all cases, as demonstrated by the influence of temperature on the surface properties of polar and n-alkane molecules. Such temperature-dependent variations can lead to inaccurate results when evaluating surface properties using IGC. The newly developed method enabled us to determine the polar enthalpy and entropy of polar model organic molecule adsorption on a variety of solid substrates, including silica, alumina, MgO, ZnO, Zn, TiO_2, and carbon fibers. Our unique method for separating dispersive and polar free surface energy enabled us to better characterize solid materials as demonstrated by Hamieh et al. [119].

A study conducted by Legras et al. emphasized the importance of solvent selection for accurate data comparisons, as molecule orientation can influence adsorbent-adsorbate interactions [120]. Optical microscopy revealed that flax samples with greater surface roughness exhibited higher surface area and variability. However, when long or chopped fibers were introduced into the chromatography column, the results were statistically insignificant. Another research by K. Yusuf et al. focused on examining the thermodynamic properties of butyl methacrylate-co-ethylene dimethacrylate neat monolith and a composite monolith combined with zeolitic imidazolate framework-8 [121]. IGC was employed under specific column pressure and temperature conditions to analyze the surface characteristics. Furthermore, Sreekanth et al. investigated the hydrocarbon adsorption affinities and solubility coefficients of cotton fabric, cardboard, and carpet fibers [122]. It was found that cotton fabric and cardboard exhibited substantially higher hydrocarbon adsorption affinities and solubility coefficients, likely due to the diffusion and dispersion of hydrocarbons across solid substrates. Additionally, Frauenhofer et al. observed a higher persistence of gasoline residues spiked on cardboard, providing further insights into the behavior of hydrocarbons on different surfaces [123]. The further advancement and implementation of IGC faces several fundamental challenges. One of these challenges is the discrepancy in reported molecular areas for polar probe molecules such as dichloromethane, acetone, ethyl acetate, tetrahydrofuran, and ethanol. Inaccurate values found in the literature are compared to the values listed in Smallwood's Handbook of Organic Solvent Properties, and this work highlights the discrepancies and provides the correct molecular area values for 11 polar probes. For example, the correct molecular areas for dichloromethane, trichloromethane, acetone, ethyl acetate, diethyl ether, and tetrahydrofuran are determined as 38.0, 44.0, 42.5, 48.0, 47.0, and 45.0 square angstroms, respectively, as reported by Shi et al. [124].

The surface characteristics of porous glass are identified using IGC. By employing IGC-ID, the dispersive component of surface energy (γ_s^d), enthalpy, and entropy of adsorption of C_6–C_{10} hydrocarbon probes are measured across a temperature range of 30–120 °C. IGC at finite concentration (IGC-FC) is utilized to obtain adsorption isotherms for *n*-octane and isopropanol probes, and subsequently, the BET specific surface areas are determined. Bauer et al. estimate the surface heterogeneity of the examined porous glasses (PGs) [125]. The effects on both types of polymer surfaces are investigated using IGC-ID to analyze the behavior of the treatment gas (He or N_2) and exposure time from one to 4 min. The adsorption of n-alkanes reveals that non-oxidative plasma treatments result in low-energy surfaces for poly (*p* -phenylene benzobisoxazole) PBO and energetically heterogeneous surfaces for poly (*p* -phenylene terephthalamide) PPTA, as reported by Martínez et al. [126].

Frauenhofer et al. described the sorption and diffusion of hydrocarbons into polydimethylsiloxane (PDMS) in the headspace-solid phase microextraction (HS-SPME) sample procedure [127]. They utilized six hydrocarbons as molecular probes and two types of non-cross-linked PDMS with different average molecular weights as stationary phases. The study conducted by B. P. Kumar et al. focused on the synthesis of nitrogen-doped multi-walled carbon nanotubes (N-MWCNTs) grafted with Sodium-carboxy methyl cellulose (Na-CMC) hybrid composite using a thermal reduction approach [128]. The hybrid composites were characterized and compared to Na-CMC particles using IGC, employing 14 different IGC methods. The results revealed that the free energy of adsorption of various solvents on the N-MWCNTs-Na-CMC surface was equivalent to the sum of the free enthalpies of the solvents individually adsorbed on the N-MWCNT and Na-CMC surfaces.

Shi et al., in 1982, introduced Gutmann's acceptor and donor number parameters to IGC, which has since become a key technology for measuring the surface Lewis acid-base characteristics of solid substances [129]. However, it is crucial to go beyond describing material qualities and use these parameters to anticipate material properties, thus advancing IGC technology. In this study, an overview of the conventional role of acid-base parameters and introduce the Schultz and Abraham methods for measuring acid-base properties. Furthermore, we explore a potential new application of IGC by establishing a relationship between the ratio of acid-base constants, K_a/K_b, and the triboelectric charge density of various polymers. Additionally, Lee et al. employed IGC-ID to determine the London dispersive and specific polar components, as well as the Lewis acid-base character of the surface free energy of graphene materials such as graphene oxide (GO), reduced graphene oxide (rGO), and graphite [130]. These surface characteristics are influenced by oxygen moieties, flaws, and micropores present in the carbon frameworks.

Adam Volkel et al. provided a comprehensive review on IGC characterization of various materials including resins, resin-based abrasive materials, polymer systems, and dental restoratives [131]. They discussed the use of solid support with anhydrous cationic surfactants as stationary phases in IGC and evaluate the miscibility of these mixtures based on surfactant-surfactant interaction parameters. Arancibia et al. investigated the thermodynamic miscibility of these systems using similar methods employed in polymeric materials [132]. Yampolskii et al. focused on the bulk sorption of small molecular load chemicals in polymers, discussing the determination of solubility coefficients, sorption isotherms, and vapor diffusion coefficients using chromatographic techniques [133]. They also examine the thermodynamic properties of glassy polymers near the glass transition and explore IGC as a probe technique for measuring free volume in polymers. Rahman et al. conducted surface energy analysis of powdered films of pH-sensitive polymers using IGC [134]. They found a strong relationship between surface energy and relative humidity in these polymeric films and coated tablets, highlighting the impact of moisture on the surface properties. The study also investigates the release of the phthalyl group from the polymer films. Klein et al. evaluated a novel IGC technique called the film cell module, which allows for the analysis of surface properties of monolithic thin solid films [135]. They compared this technique with traditional IGC, which typically analyzes powder samples, fibers, and polymer-coated substrates. The surface energy of four different solid supports was measured using both traditional IGC and the film cell module or the sessile drop approach with samples in the film state.

Zhang et al. highlighted the significant impact of adhesion between fiber reinforcement and matrix on the performance of composite materials, particularly the role of surface characteristics of silk fibroin in determining adhesion levels in cocoons [136]. The study investigated the mechanical properties of silk cocoons and silk fibroin, revealing surface energy heterogeneity of the fibers through IGC studies. Ramanaiah et al. examined the surface energetics of gabapentin (GBP) and pregabalin (PGB) using a surface energy analyzer (SEA) based on IGC [137]. The research found that these medications, despite having distinct structures, exhibited primarily basic surfaces based on their higher surface Lewis base parameter (K_b). The temperature dependency

of the Lewis acid-base characteristics was attributed to the breakdown of intramolecular hydrogen bonding at higher temperatures. Xia et al. developed a modified model considering temperature influence on group interactions for polydimethylsiloxane PDMS [138]. IGC was used to determine interaction parameters between common groups in PDMS, and the model showed good agreement with experimental data. The model was also utilized to calculate partition equilibrium between acetone/butanol/ethanol water solutions and PDMS with varying polymerization degrees and side chain length, aiding in the development of the UNIFAC-ZM model and guiding separation procedures of silicone polymer complexes. Avgidou et al. focused on understanding the surface thermodynamics of swine intestinal mucin using IGC-ID and a temperature range below the glass transition [139]. The study evaluated the affinity of various chemical probes to the mucin surface in terms of dispersive and specific interactions determined from chromatographic retention profiles, achieving well-defined Gaussian peaks characteristic of Henry's adsorption, for the first time.

According to Hadjittofis et al. IGC is a well-established technique for determining surface energy, particularly in heterogeneous materials like particulate and fibrous materials, [140]. However, variability in sample and column preparation can lead to low data repeatability. The authors investigated two factors of chromatographic column preparation, namely the amount of silanised glass wool and the packing structure of mixtures of particulate materials, using a combined experimental and modeling approach to understand their impact on IGC measurements. Zhao et al. examined the fabrication of alkali lignin/PVA composite membranes by incorporating different percentages of alkali lignin [141]. The thermodynamic characteristics of the composites were measured using IGC. The study found that the composite membrane with a 15% alkali lignin content exhibited a tensile strength of 18.86 MPa and a hydrophilic contact angle of 89°. The solubility parameters of the blends were found to be correlated with the mechanical and hydrophilic properties of the composites, and this correlation was empirically and theoretically validated. Chen et al. used the IGC method to investigate the solubility parameters and surface parameters of two types of common alcoholysis, polyvinyl alcohol (PVA), PVA88 and PVA99 [142]. The accuracy of the IGC experiment's solubility parameters was confirmed by molecular dynamics modeling. The study aimed to determine the suitable PVA chain length for simulation verification computation by examining the influence of repeated units of PVA on solubility characteristics. The results showed that when the PVA chain length was 30 V and above, the solubility parameters did not differ significantly, and the numerical trends matched the results of molecular dynamics simulation. Kanatieva et al. employed IGC to examine the chromatographic characteristics of capillary columns constructed with polymers of varied backbone architectures, demonstrating the feasibility of polymer differentiation. Two new stationary phases were created using different polymerization methods [143]. The comparison of the separation and adsorption capabilities of these novel phases with conventional GC stationary phases revealed their non-polar nature. Legras et al. described the dispersive and acid-base surface energy profiles of flax and kenaf fibers, as well as cellulose B fibers produced by a dry jet, wet spinning technique [144]. The study utilized IGC by injecting a series of n-alkanes at finite dilution to obtain the dispersive energy distribution profile at 30 °C and 0% RH. The acid-base contributions were determined using the Van Oss method and injection of monopolar probes. The cellulose B fibers exhibited the most homogeneous surface energy, while the bast fibers showed higher polar components and broader surface energy distributions compared to the cellulose fibers. Adiguzel et al. synthesized and investigated a diethanol amine modified polystyrene-based polymer (PVBC-Diethanol amine) using IGC-ID [145]. Retention diagrams were constructed across a temperature range to analyze the interaction of polar and nonpolar probes with the polymer. The measurements of K_a and K_b indicated that the PVBC-Diethanol amine surface was basic.

Bilgiç et al. employed IGC to characterize the surface of kaolinite [146]. By analyzing the retention time of various non-polar and polar probes at infinite dilution, they estimated the adsorption thermodynamic parameters like standard enthalpy (ΔH_a^S), entropy (ΔG_a^S), and free energy of adsorption (ΔG_a^d), as well as the dispersive component of the surface energy (γ_s^d), and the acid/base character of the kaolinite surface. These measurements provided insights into the surface properties of kaolinite. According to Yu et al. blast furnace slag (BFS), sulphoaluminate cement (SAC), and Portland cement (PO) were carefully analyzed using IGC to investigate the dispersive component, specific surface free energy, and acid-base characteristics associated with these binding materials [147]. The results revealed that a significant portion of the surface free energy in all three binding materials is attributed to the dispersive component, indicating relatively low polarity. The analysis of acid-base characteristics indicated that the surfaces of all three samples exhibit basic properties. Additionally, the adsorption experiment demonstrated that BFS exhibited the highest adsorption of superplasticizer molecules per unit surface, suggesting that higher surface free energies facilitate superplasticizer adsorption.

Hamieh et al. employed IGC to calculate the acid-base surface properties of various solid substrates, including oxides, polymers, and polymers adsorbed on oxides [148]. In another study by Hamieh et al. the specific entropy of poly (-*n*-alkyl) methacrylates adsorbed on silica or alumina, as well as in their bulk phases, was investigated using IGC [149]. The free enthalpy of adsorption for polar molecules at different temperatures was computed for the polymers studied. This allowed for the determination of the specific enthalpy and entropy of polar probes adsorbed on these polymers, whether in their adsorbed state on alumina and silica or in their bulk phase. The results showed that the length of the alkyl group within the poly (-*n*-alkyl) methacrylates chain significantly influenced the specific entropy. According to Hamieh et al. a study on the surface properties of PMMA/SiO_2 and PMMA/Al_2O_3 revealed significant differences in the physicochemical behavior of oxides covered with varying concentrations of PMMA [150]. The investigation also highlighted the impact of polymer tacticity on the specific entropy of PMMA adsorbed on oxides. Lastly, Hamieh et al. evaluated the acid-base characteristics of Poly (α-*n*-alkyl) methacrylates in Lewis terms when adsorbed on silica. They computed the acid-base constants K_a and K_b of various polymers by applying the traditional model and proposing a novel model that includes a third constant, K to account for the amphoteric nature of the solid substrates. This novel model provided more accurate and quantifiable results. Changes in the length of the alkyl group in the side chain of Poly (α-*n*-alkyl) methacrylates resulted in variations in the surface properties of these polymers, impacting all surface characteristics, particularly the acid-base constants and transition phenomena.

Kumar et al. presented a study on the gas sensing performance of an oligoacenaphthylene (OAN)/p-hydroxyphenylacetic acid (*p*-HPA) composite at room temperature [151]. The London dispersive surface energy γ_s^d is determined using 14 representative models based on IGC. The results indicate that both OAN and the OAN/p-HPA composite exhibit higher Lewis basic characteristics, with the OAN/p-HPA surface demonstrating higher basicity compared to OAN alone. The incorporation of phenolic groups in the composite enhances its ability to sense CO gas, showing a sensitivity of 8.96% and good cycle stability compared to the pure components. This work sheds light on a novel approach for investigating polymer composite materials for future applications. In another study by Kumar et al. the surface thermodynamics of the polymer, Poly (vinylidene chloride-*co*-acrylonitrile) (P(VDC-*co*-AN)) in its pure state was characterized using IGC technique [104]. Various IGC properties of the polymer, including the London dispersive surface energy, Gibbs free energy, and Guttman Lewis acid-base parameters, were investigated. The Schultz and Dorris-Gray methods were employed to calculate the London dispersive surface free energy (LS), but their methods were criticized and corrected by Hamieh et al. that proved the variations of the surface area of organic molecules as a function of the

temperature. Additionally, the visual properties of the polymer were studied using CVIP techniques. Detailed patterns, surface morphology, texture/roughness, particle area distribution (DA), directionality (DP), mean average particle area (avg), and mean average particle standard deviation (avg) were among the visual features investigated in the pure form of the Poly (vinylidene chloride-*co*-acrylonitrile) polymer. This collaborative study provides insights into the chemical and visual aspects of the pure form of the polymer, Poly (vinylidene chloride-*co*-acrylonitrile) (P(VDC-*co*-AN)), enabling researchers to explore its properties comprehensively.

Introducing to Kumar et al. this study introduces new advancements in surface thermodynamic methods for determining the London dispersive surface free energy component, specific free energy of adsorption, and Lewis acid-base properties of polymers using IGC-ID [152]. The IGC technique was utilized to measure the net retention volumes V_N of n-alkanes and polar solvents adsorbed on a sodium carboxymethyl cellulose (Na-CMC) polymer surface at four different temperatures. Various models, including Dorris-Gray, Dorris-Gray-Hamieh, van der Waals, Redlich-Kwong, Kiselev, geometric, cylindrical, spherical, and Hamieh models, were employed to calculate the London dispersive surface free energy component of Na-CMC. The study demonstrated that different IGC approaches and models yield non-comparable results. The thermal model yielded the most accurate Lewis acid-base characteristics of the Na-CMC surface. In another work by Kumar et al., single-walled carbon nanotubes (SWCNTs) and a SWCNT-polytetrafluoroethylene (PTFE) blend were synthesized using a simple reaction mixture and chromosorb (SiO_2) [153]. Additionally, IGC is employed to evaluate the surface thermodynamic characteristics of n-alkanes and the net retention volumes of polar probes. This study reveals that the surface of the (SWCNT-PTFE) blend contains more acidic sites compared to the SWCNT surface. Therefore, the IGC data provide valuable additional insights into the surface properties of the (SWCNT-PTFE) blend.

In a study conducted by Rani et al. IGC was used to assess the net retention volumes, V_N of n-alkanes and five polar solute probes on cellulose acetate butyrate - polycaprolactonediol. The V_N values of the five polar solutes were utilized to calculate the specific components of adsorption enthalpy and entropy [154]. The objective of the paper by Kumar et al. is to investigate the impact of an excipient on the surface energetics of the Efavirenz (EFV) medication [155]. IGC was employed to determine the net retention volumes V_N for n-alkanes and polar solutes on two columns: one containing EFV drug and the other a blend of EFV and cellulose acetate propionate. The K_a values for EFV and the blend were nearly identical, while the K_b values were higher for EFV than the blend. Both methods showed a similar trend in K_a and K_b. The objective of the paper by Kumar et al. is to investigate the surface energetics of the polymer excipient cellulose acetate propionate (CAP) in its solid form [156]. Table 1 presents the IGC-determined characteristics of polymers, copolymers, and their composites.

4.2. Surfactants

Surfactants are essential in surface chemistry as they act as surface-active agents, adsorbing at interfaces and reducing surface tension. They are classified as cationic, anionic, or non-ionic based on the type of polar group they possess. The thermodynamic properties of these surfactants were found to be affected by temperature, molecule structure, molecular weight, chain length, component ratio, polarity, and hydrogen bonding components. In a study by Voelkel et al. IGC was employed to investigate the binary parameters resulting from hydrogen bonding and polarity of 1-hexadecanol oxyethylene derivatives [157]. The use of two sets of polar probes capable of forming hydrogen and polar bonds allowed the researchers to conclude that the structure of the liquid stationary phase (oxyethylate) and the temperature of the IGC column could contribute to changes in hydrogen bonding and polar binary parameters. However, no general correlation was identified between these two characteristics and

Table 1
IGC physicochemical properties of polymers, copolymers and their composites.

Parameter	Compound	References
Dispersive Surface free energy	Polytetrafluoroethylene; kenaf cellulose; Melamine and thiourea-derived graphitic carbon nitrides; 3-mercaptopropyltrimethoxysilane; Poly (*p*-phenylene terephthalamide) (PPTA) and poly (*p*-phenylene benzobisoxazole); nitrogen doped multi walled carbon nanotubes (N-MWCNTs) grafted Sodium-carboxy methyl cellulose; graphene oxide and reduced graphene oxide; hypromellose phthalate (HPMCP) and methacrylic acid copolymer; Gabapentin (GBP) [2-[1-(aminomethyl) cyclohexyl] acetic acid] and Pregabalin (PGB) [(S)-3 (aminomethyl)-5-methylhexanoic acid]; nickel hydroxide into Ni (OH)2 nanosheets; PVA88 and PVA99; polystyrene based polymer (PVBC-Diethanol amine); kaolinite; furnace slag (BFS); sulphoaluminate cement (SAC) and portland cement (P·O), Monogal; MgO and ZnO; poly (methylmethacrylate)(PMMA); polytetrafluoroethylene.	[119,120,122, 125,126,128,130, 134,137,142, 144–150]
Surface Area	Polytetrafluoroethylene; kenaf cellulose; Melamine and thiourea-derived graphitic carbon nitrides; poly (*p*-phenylene terephthalamide) (PPTA) and poly (*p*-phenylene benzobisoxazole); nitrogen doped multi walled carbon nanotubes (N-MWCNTs) grafted Sodium-carboxy methyl cellulose; Cellulose B; crystalline 5-((S)-3,7-Dimethyloctyloxy)-2-[[[4-(dodecyloxy) phenyl] imino] methyl] phenol (DODPIMP); furnace slag (BFS); sulphoaluminate cement (SAC) and portland cement (P·O); Monogal; MgO and ZnO; polytetrafluoroethylene.	[119,120,122, 126,128,144,145, 147,148,150]
Enthalpy of Adsorption	Melamine and thiourea-derived graphitic carbon nitrides; 3-mercaptopropyltrimethoxysilane; poly (*p*-phenylene terephthalamide) (PPTA) and poly (*p*-phenylene benzobisoxazole); nitrogen doped multi walled carbon nanotubes (N-MWCNTs) grafted Sodium-carboxy methyl cellulose; graphene oxide and reduced graphene oxide; PVA88 and PVA99; Cellulose B; polystyrene based polymer (PVBC-Diethanol amine); Crystalline 5-((S)-3,7-Dimethyloctyloxy)-2-[[[4-(dodecyloxy) phenyl] imino] methyl] phenol (DODPIMP); kaolinite; furnace slag (BFS); sulphoaluminate cement (SAC) and portland cement (P·O); Monogal; MgO and ZnO; poly (methylmethacrylate)(PMMA); polytetrafluoroethylene	[122,125,126, 128,130,137, 144–150]
Entropy of Adsorption	Melamine and thiourea-derived graphitic carbon nitrides; poly (*p*-phenylene terephthalamide) (PPTA) and poly (*p*-phenylene benzobisoxazole); nitrogen doped multi walled carbon nanotubes (N-MWCNTs) grafted Sodium-carboxy methyl cellulose; graphene oxide and reduced graphene oxide; PVA88 and PVA99; Cellulose B; polystyrene based polymer (PVBC-Diethanol amine); crystalline 5-((S)-3,7-Dimethyloctyloxy)-2-[[[4-(dodecyloxy) phenyl] imino] methyl] phenol (DODPIMP); kaolinite; furnace slag (BFS); sulphoaluminate cement (SAC) and portland cement (P·O); Monogal; MgO and ZnO; poly (methylmethacrylate)(PMMA); polytetrafluoroethylene	[122,125,126, 128,134,137, 144–150]
Acid Base Properties	Melamine and thiourea-derived graphitic carbon nitrides; 3-mercaptopropyltrimethoxysilane; poly (*p*-phenylene	[122,125,126, 128,130,137, 145–150]

(*continued on next page*)

Table 1 (*continued*)

Parameter	Compound	References
	terephthalamide) (PPTA) and poly (*p*-phenylene benzobisoxazole; crystalline 5-((S)-3,7-Dimethyloctyloxy)-2-[[[4-(dodecyloxy) phenyl] imino] methyl] phenol (DODPIMP); nitrogen doped multi walled carbon nanotubes (N-MWCNTs) grafted Sodium-carboxy methyl cellulose; graphene oxide and reduced graphene oxide; Gabapentin (GBP) [2-[1-(aminomethyl) cyclohexyl] acetic acid] and Pregabalin (PGB) [(S)-3-(aminomethyl)-5-methylhexanoic acid]; Cellulose B; polystyrene based polymer (PVBC-Diethanol amine); kaolinite; furnace slag (BFS); sulphoaluminate cement (SAC) and portland cement (P·O); Monogal; MgO and ZnO; poly (methylmethacrylate)(PMMA); polytetrafluoroethylene.	

column temperature.

According to Reddy et al. the dispersive component of surface free energy γ_s^d, of Amberlite XAD-4 was calculated using IGC and the net retention volumes (V_N) of n-alkanes at different temperatures [158]. The results showed that the γ_s^d values decrease as temperature increases. Furthermore, the specific components of free energy of adsorption (ΔG_a^S) and enthalpy of adsorption (ΔH_a^S) were determined using the V_N values of acid-base probes. The Donnet method, considering the molar deformation polarization of solutes, was utilized for evaluating ΔG_a^S. In another study by Kumar et al. the surface thermodynamic properties of Amberlite XAD-7 acrylic-ester-resin were investigated using IGC-ID [105]. The London dispersive surface free energy was estimated using various models, including the Fowkes equation, Dorris-Gray relation, Hamieh-Dorris-Gray model, and six other molecular models based on the surface areas of organic molecules. Additionally, the Hamieh model, considering the thermal effect, was used. It was observed that the London dispersive surface free energy values decrease with increasing temperature, regardless of the methodology or model employed.

4.3. Pharmaceutical powders

Pharmaceutical powders are a highly studied subject in the field of IGC, especially after polymers. The pharmaceutical industry requires precise characterization of small quantities of substances in various forms such as amorphous, polymorphs, hydrates, co-crystals, and solvates. This is crucial for understanding interactions between multiple active ingredients in a product. Additionally, the surface energy distribution of pharmaceutical powders, which are often energetically heterogeneous, significantly impacts product quality. Traditional methods like contact angle measurements are believed to be influenced by experimental conditions, leading to potential interference with results [159]. Therefore, there has been a growing interest in using IGC for surface characterization of active pharmaceutical ingredients (APIs), excipients, and drug delivery systems (DDS). IGC has proven to be an effective tool in predicting storage conditions and shelf life of pharmaceuticals by assessing the crystallization rates of amorphous dispersions [160]. This advancement in IGC techniques provides valuable insights for the pharmaceutical industry and facilitates better understanding and control of pharmaceutical powder properties.

Strzemiecka et al. conducted a study on the effect of humidity on material characteristics [161]. They investigated how humidity impacts the surface properties of materials using IGC. Das et al. focused on understanding the de-agglomeration of lactose by exploring the powder strength distributions of a cohesive bed [162]. Their aim was to gain insights into the process and mechanism of lactose de-agglomeration. Ho et al. investigated the influence of milling on particle shape and surface energy heterogeneity of needle-shaped crystals [163]. They found that particle shape plays a significant role in the milling process and affects fracture behavior. Gamble et al. utilized IGC to compare surface energy analysis as a method for probing the surface energy properties of micronized materials [164]. This study aimed to understand the surface energy characteristics of micronized particles. Zhou et al. focused on modifying lactose carrier surfaces to study drug-lactose binding characteristics in adhesive mixtures and control performance in dry powder inhaler formulations [165]. They explored the possibility of modifying the surface properties of lactose for better drug delivery. Their study aimed to gain insights into the acid-base properties of kaolinite surfaces. These studies demonstrate the diverse applications of IGC in characterizing solid surfaces and investigating various factors that influence surface properties, such as humidity, particle shape, drug-lactose interactions, and acid-base features. IGC provides a valuable tool for understanding and controlling surface properties of materials in different applications.

Koodziejek et al. conducted a study to explore the relationship between surface characteristics, determined by IGC, and the release of ibuprofen from fumed silica-based hybrid materials [166]. They investigated how the surface properties of the materials influence drug release. Gamble et al. used IGC to examine the impact of micronization on the surface energy properties of an active pharmaceutical ingredient (API) called Ibipinabant [167]. Their study focused on understanding the changes in surface energy caused by the micronization process. Das et al. employed IGC to determine the polar and total surface energy distributions of particles [168]. They aimed to analyze the surface energy characteristics of the particles using IGC. They have investigated the application of IGC in studying mechanofusion processing and the behavior of lactose coated with magnesium stearate [169]. They used IGC to gain insights into the surface properties of the lactose particles and their interactions with the coating material. Zhou et al. studied the surface characteristics of a model pharmaceutical fine powder treated with a pharmaceutical lubricant to enhance flow using a mechanical dry coating technique [170]. They employed IGC to analyze the changes in surface properties induced by the coating process. Das et al. analyzed the surface energy characterization of medicinal powders using IGC-FD [171]. They examined how humidity affects the surface properties and behavior of the mixtures using IGC. The scientific points above-covered researches involve studying the surface characteristics and interactions of pharmaceutical materials, investigating the impact of particle size reduction, characterizing surface energy distributions, analyzing surface modification techniques, understanding the behavior of mixtures during storage, and exploring the surface energy properties of medicinal powders.

Das et al. conducted a study using IGC to analyze the changes in surface energy of lactose during storage. By measuring surface energy, they gained insights into the behavior of lactose over time [172]. Matthew et al. investigated the application of IGC for studying lactose and medicinal components used in dry powder inhalers [173]. They explored the use of IGC to understand the surface properties and interactions of these materials. Miyanishi et al. utilized IGC to assess the crystallization behavior on the surface of Nifedipine solid dispersion powder [174]. They used IGC as a tool to investigate the disorder in the materials. Hamieh et al. aimed to determine the Lewis acid-base characteristics of Poly (α-*n*-alkyl) methacrylates adsorbed on silica using IGC. Their study focused on understanding the acid-base properties of the adsorbed polymers [175]. Their study aimed to enhance the understanding and interpretation of IGC results using computational modeling. Ho et al. examined the surface heterogeneity of D-mannitol using sessile drop contact angle and finite concentration IGC [176]. They focused on understanding the surface properties and heterogeneity of D-mannitol using these techniques. Wang et al. published a study investigating the surface properties of solid materials using modified IGC [177]. They utilized IGC to assess the surface characteristics of the materials and gain insights into their properties. Das et al. utilized IGC to

study mechanofusion processing and the behavior of lactose coated with magnesium stearate [178]. They examined how the surface properties of powders contribute to their functionality in pharmaceutical applications. the scientific points covered in above references range from studying the changes in surface energy during storage, exploring surface properties and interactions, assessing crystallization behavior, investigating disorder in milled materials, determining acid-base characteristics, understanding the role of surface energetics in drug delivery, utilizing molecular modeling for data interpretation, analyzing surface heterogeneity, exploring modified IGC techniques for surface characterization.

Koodziejek et al. conducted a study using IGC to investigate the surface features of hybrid materials, which have the potential to be carriers for sustained release of active drugs [179]. This research contributes to understanding the surface properties of these materials and their suitability for drug delivery applications [179]. Shi et al. published a study that focuses on enhancing the calculation accuracy of acid-base constants using an IGC approach [180]. By improving the accuracy of these calculations, researchers can gain a deeper understanding of the acid-base properties of materials, which is essential for various applications such as drug formulation and chemical reactions. Jones et al. employed inverse gas chromatography to study lactose and medicinal components used in dry powder inhalers [181]. This research helps in understanding the surface properties and interactions of these components, which is crucial for optimizing the performance and efficacy of inhalation drug delivery systems. Zhou et al. conducted a study investigating drug-lactose binding characteristics in adhesive mixes and modulating performance in dry powder inhaler formulations by modifying lactose carrier surfaces [182]. This research offers insights into the surface modification of lactose carriers to improve drug-lactose interactions and enhance the performance of dry powder inhalers. Bilancetti et al. utilized spray drying to prepare starch particles for use in a dry powder coating technique [183]. The study demonstrates the application of spray drying in preparing particles with specific surface characteristics, which is relevant for various coating and formulation processes in the pharmaceutical industry. This research contributes to understanding the dynamic changes in surface energy over time, providing insights into surface properties and interactions in complex systems. Brum et al. reported on the utilization of dispersive surface energy in estimating surface amorphous content and developed the concept of effective amorphous surface area [184]. This research offers a method to estimate the amorphous content of materials based on their surface energy, which is valuable for characterizing and predicting the stability and behavior of amorphous formulations. Burnett et al. investigated the effect of processing procedures on the surface characteristics of amorphous indomethacin using IGC [185]. This study examines how different processing methods impact the surface properties of amorphous materials, providing insights into formulation and processing optimization. Overall, the scientific value of these references lies in their contribution to understanding surface features, surface modification techniques, surface energy analysis, and the impact of processing procedures on the surface characteristics of pharmaceutical materials. This knowledge is essential for formulating effective drug delivery systems, optimizing drug performance, and predicting the behavior and stability of pharmaceutical formulations.

This research offers valuable information on the impact of processing and environmental conditions on the surface characteristics and stability of pharmaceutical compounds. Ke et al. conducted a study on the effect of preparation procedures on the surface/bulk molecular mobility and glass fragility of solid dispersions [186]. This research sheds light on the influence of spray drying conditions on the physical stability of amorphous formulations, which is essential for developing stable pharmaceutical products. Le et al. used IGC to investigate the effect of lactose grade in dry powder formulations of fluticasone propionate and terbutaline sulphate [187]. This study explores the impact of lactose characteristics on the surface properties and performance of dry powder formulations, contributing to formulation optimization. Ho et al. examined the effect of fines on lactose surface energy heterogeneity for pulmonary medication delivery [188]. This research provides insights into the impact of particle size distribution and surface properties of lactose on its performance as a carrier in dry powder inhalers. Shariare et al. investigated the effect of material properties and process parameters on lactose monohydrate micronization [189]. This study explores the occurrence and implications of disorder in crystalline materials, enhancing the understanding of their physical properties and behavior. The scientific value of these references lies in their contributions to the understanding of surface properties, stability, formulation, and processing of pharmaceutical powders. They provide valuable insights into the surface energy, acid-base interactions, batch variation, stability, and the impact of different factors on the surface characteristics of powders. This knowledge is crucial for optimizing formulation performance, ensuring consistent quality, and enhancing the understanding of powder behavior in pharmaceutical applications.

This finding is scientifically valuable as it provides insights into the surface properties and energetics of lactose mixes, helping to understand their behavior and stability. Miyanishi et al. used IGC to study the crystallization behavior on the surface of an amorphous solid dispersion powder and predict its physical stability at temperatures below the glass transition temperature, Tg [190]. This finding has scientific value as it offers a potential method for assessing the suitability of powders for inhalation formulations based on their surface characteristics, which can impact their dispersibility and performance. Peng et al. investigated the effect of drying methods on the surface energy of cellulose nanofibrils (CNFs) [191]. By using IGC, they explored the impact of different drying processes on the surface properties of CNFs. This research contributes to the understanding of the drying-induced changes in the surface energy of nanocellulosic materials, which is important for their formulation and application development. Kolakovic et al. emphasized the versatility of nanofibrillar cellulose (NFC) as an excipient for pharmaceutical dosage forms and highlighted the need for further research to fully explore its potential in pharmaceutical applications [192]. This research provides insights into the surface characteristics of lactose, which is valuable for understanding its behavior and optimizing its use in pharmaceutical formulations. Tay et al. found that magnesium stearate improves the dispersion of salbutamol sulphate (SS) [193]. Their goal was to understand the mechanism behind the enhanced respiratory deposition of SS with the addition of magnesium stearate. This study contributes to the understanding of the surface properties and interactions between SS and magnesium stearate, offering insights into their formulation and performance.

This study is scientifically valuable as it contributes to the understanding of surface properties of lactose and provides insights into the consistency and reliability of theoretical models in interpreting experimental data. Han et al. investigated the effect of Ibuprofen on the passivation/stabilization of high-surface-energy sites [194]. This research is scientifically valuable as it explores the interaction between Ibuprofen and high-surface-energy sites, contributing to the understanding of drug-surface interactions and potential stabilization mechanisms. Kumar et al. highlighted the use of surface thermodynamic properties to understand the interaction potential between drug surfaces and excipients in the formulation and drug release process [195]. This perspective is scientifically valuable as it emphasizes the importance of surface energetics in formulating effective drug delivery systems. Kumar et al. used IGC to measure the retention volumes of n-alkanes and polar probes on the drug surface of 2-hydroxypyrimidine sulphate (2-HPS) [196]. This study contributes scientific value by providing insights into the surface properties and energetics of 2-HPS, aiding in the understanding of its behavior and potential applications. Kumar et al. employed IGC to determine the dispersive surface free energy of a fluconazole powder surface at different temperatures [197]. This research is scientifically valuable as it explores the surface energetics of fluconazole and provides insights into its surface characteristics and potential

interactions with other substances. Esim et al. aimed to develop a time-controlled medication delivery system for telmisartan [198]. This research is scientifically valuable as it addresses the challenge of limited water solubility of telmisartan and explores solid dispersion processes to enhance its solubility and create chronotherapeutic tablets. Overall, these studies provide scientific insights into various aspects of surface properties, interactions, stability, and formulation of pharmaceutical materials. They contribute to the understanding of surface energetics, surface characterization, drug-surface interactions, and the development of innovative drug delivery systems. Table 2 presents the characteristics of pharmaceutical powders and their hybrid composites as determined by IGC.

4.4. Minerals and organic-inorganic compounds

Surface characterization of minerals, particularly those with high surface energy, can be challenging due to their tendency to adsorb water. However, IGC method has proven effective in characterizing such materials. One example is the use of IGC-ID to investigate the surface properties of calcium carbonate ($CaCO_3$), a high-energy surface filler [199]. The study revealed that the strongly basic surface of $CaCO_3$ was significantly reduced in basicity when coated. This change in acidity was attributed to the heterogeneous distribution of the coating and the presence of surfactant coverage exceeding a monolayer on the surface [200]. In another study, Keller and Luner compared the surface chemistry of synthetic calcium carbonate, marble, and chalk, focusing on porosity, BET surface area, and chemical composition [201]. The results showed that the surface energetics of calcium carbonates are greatly influenced by the presence of physically and chemically adsorbed water on the surface and within the pores. The dehydration of the material caused an increase in surface energy. The IGC method demonstrated high sensitivity in monitoring water desorption, even at sub-monolayer concentrations. Overall, the application of IGC in these studies has provided valuable insights into the surface properties and behavior of minerals, shedding light on the effects of coating, hydration, and dehydration on their surface energy and chemistry.

Table 2
IGC physicochemical properties of Pharmaceutical powders and their composites.

Parameter	Compound	References
Surface Free Energy	Perlite; Lactose; β polymorph of D-mannitol; Ibipinabant, coarse lactose; untreated kaolinite and kaolinites; ibuprofen; silicon dioxide; PharmatoseP450; lactose coated with magnesium stearate; fine lactose powder; magnesiumstearate; nifedipine and polyvinylpyrrolidon (PVP) K-30; coarse lactose (CL) and micronized lactose (ML); starch; dry powderinhalerformulations (DPIs); Ibuprofen micronization cefditorenpivoxil powder; D-mannitol; fluticasone propionate and terbutaline sulphate; Lactose monohydrate; salbutamol sulphate; salbutamol sulphate; budesonide; and formoterol fumarate dihydrate; α-lactose monohydrate; Ibuprofen micronization; Phenylpropanolamine; 2-hydroxypyrimidine sulphate; Fluconazole.	[161,163–165, 165–172,175,178,181, 183,185,187–190, 193–196],]197]
Surface Area	Perlite; Lactose; β polymorph of D-mannitol; Ibipinabant, coarse lactose; untreated kaolinite and kaolinites; ibuprofen; silicon dioxide; PharmatoseP450; lactose coated with magnesium stearate; fine lactose powder; magnesiumstearate; nifedipine and polyvinylpyrrolidon (PVP) K-30; coarse lactose (CL) and micronized lactose (ML); starch; dry powderinhalerformulations (DPIs); Ibuprofen micronization cefditorenpivoxil powder; D-mannitol; fluticasone propionate and terbutaline sulphate; Lactose monohydrate; salbutamol sulphate; salbutamol sulphate; budesonide; and formoterol fumarate dihydrate; α-lactose monohydrate; Ibuprofen micronization; Phenylpropanolamine; 2-hydroxypyrimidine sulphate; Fluconazole.	[161,163–165, 165–172,175,178,181, 183,185,187–190, 193–196],]197]
Acid Base Properties	Ibipinabant; coarse lactose; ibuprofen; magnesiumstearate; dry Phenylpropanolamine.	[161–163,167,185]
Relative Humidity	Perlite	164

4.5. Zeolites

Natural zeolites are widely used in various applications due to their unique porosity and high specific surface area. They find use as catalysts, for gas separation, ion exchange, and as selective molecular sieves for separating components of mixtures. Additionally, they serve as adsorbents in water treatment and purification of industrial fluids. In the characterization of zeolites, IGC has been employed to investigate surface free energy, adsorption properties, and the influence of storage conditions [202–204]. IGC studies on zeolites have revealed that surface acidity and basicity are directly related to the relative humidity of the carrier gas. However, fine and thick zeolites with high activity posed challenges in evaluating related parameters. Furthermore, IGC has facilitated research on the utilization of zeolites in the production of abrasive materials without the need for trial products, leading to time and cost efficiency [205]. In examining the effect of various acids, aqueous solutions, and model post-fermentation broth on the surface properties of Zeolite 5A, IGC was used to compare it with other sorbents such as Amberlite XAD7HP and Diaion SK116. Zeolite 5A exhibited the most acidic surface, and significant changes in dispersive surface energy were observed due to water adsorption during impregnation, which obstructed the zeolite's active sites [206]. Additionally, IGC has been employed to evaluate fragrance adsorption on natural and synthesized zeolites, as the BET technique alone was insufficient for surface characterization and predicting adsorption behavior [207]. Thielmann et al. utilized thermal desorption methods in conjunction with IGC to examine the surfaces of 3A and 13*X* zeolites, enabling the distinction between micropore and mesopore contributions to adsorption phenomena based on differences in adsorption mechanisms [208]. These IGC studies have provided valuable insights into the surface properties, adsorption behavior, and utilization of zeolites in various applications, contributing to the understanding and optimization of zeolite-based materials.

4.6. Nanomaterials

Nanomaterials belong to the aforementioned material classes but possess unique nanostructures that differentiate them from bulk materials. Due to their small particle size, nanomaterials exhibit distinct chemical and physical properties, including electronic properties and surface energy. In the field of nanomaterials, IGC has primarily been applied to carbon nanoparticles, particularly carbon nanotubes (CNTs). Menzel et al. conducted a study using IGC to explore the physicochemical surface characteristics of CNTs, focusing on dispersive surface energy and surface heterogeneity [209]. Their innovative approach involved separating the investigation of surface structure and surface chemistry to avoid conflating these two aspects. IGC has proven to be a powerful method for analyzing the surfaces of CVD-grown multiwalled carbon nanotubes [210]. The study determined and compared dispersive surface energy (γ_s^d), acid and base numbers (K_a and K_b), and specific

free energy (ΔG_p^S) for various types of CNTs, including commercial, in-house, and surface-modified CNTs prepared through high temperature annealing, thermal oxidation, and grafting with methyl methacrylate.

The IGC results demonstrated good agreement with standard surface characterization techniques such as Bohm's titration, scanning electron microscopy (SEM), and X-ray photoelectron spectroscopy (XPS). As-received CNT samples exhibited high dispersive surface energy, while the commercial CNTs displayed a greater polar component compared to the graphitic in-house materials. Surface alterations through high temperature annealing decreased surface polarity, whereas thermal oxidation increased surface polarity. Additionally, the grafting of methyl methacrylate in modest quantities had a noticeable impact on the surface properties of the studied carbon nanotubes, leading to reduced surface energy and adsorption capacity. Furthermore, IGC was employed to investigate the mechanism of organic chemical adsorption on carbon nanotubes [211]. These studies utilizing IGC in the field of nanomaterials contribute to a better understanding of the surface properties, surface alterations, and adsorption behavior of carbon nanotubes, offering insights for their various applications.

4.7. Metal organic frame works

Metal-organic frameworks (MOFs), formerly known as adsorbent materials, have gained significant attention in recent years due to their potential for storing and converting thermal energy. Particularly, the utilization of MOFs-water working pairs holds promise as a groundbreaking advancement in sorption-based thermal energy storage and conversion systems. MOFs are a unique class of porous crystalline materials constructed by linking metallic nodes, such as single ions or clusters, with organic linkers. Over the past two decades, extensive research has been conducted to explore the diverse applications of MOFs, including gas storage, separation, catalysis, and sensing [212]. MOFs exhibit remarkable chemical, structural, and topological flexibility as organic-inorganic hybrid porous materials [213]. These applications leverage the controllable pore system of MOFs, allowing for on-demand manipulation of pore aperture, shape, size, and functionality to address specific challenges [214]. Through various design and engineering strategies, the pore system of MOFs can be tailored to achieve desired properties and functionalities.

MOFs offer efficient construction possibilities with tailored qualities such as pore aperture size, shape like channels or cages, and controlled by the arrangement of organic linkers connected through metallic nodes. This precise assembly of inorganic and organic building blocks, guided by reticular chemistry principles, results in hybrid material frameworks with specific topologies and geometrical information. The focus of this review is on MOFs that exhibit hydrophobic-oleophilic, hydrophilic-underwater oleophobic, and switchable wettability properties, emphasizing their potential as oil/water separators. Depending on the specific methods employed for separating oil/water mixtures and emulsions, various MOFs-based materials can be categorized as filtering materials, absorbents, or adsorbents. We discuss different subclasses of MOF-based filtration, absorbent, and adsorbent materials, highlighting recent advancements in their applications for oil/water separation. Finally, we critically examine the significance of these MOFs in oil-water separation and propose potential future approaches to enhance their performance [215].

In a separate study, IGC was utilized to characterize the surface properties of single-crystalline and polycrystalline TAPPy-PDA COFs for the separation of linear n-alkanes and a series of standard polar probes. The findings revealed significant variations in separation behavior between single-crystalline and polycrystalline 2D COFs, shedding light on the interactions between analytes and these surfaces. Analysis using McReynolds constants indicated that the surface of single-crystalline TAPPy-PDA COF is nonpolar, while the surface of polycrystalline TAPPy-PDA COF possesses some degree of polarity [216]. A green synthesis technique was employed to produce MIL-100(Fe), a highly promising MOF for efficient water sorption, as well as its transition metal-doped variants like Ni^{2+} and Co^{2+}. Thermogravimetric measurements were conducted to determine the water sorption capacity of these materials, and the experimental adsorption data were analyzed using the Sun-Chakraborty adsorption isotherm model [217]. In another study, the surface thermodynamic properties, specific interactions, and acid-base constants of crystals of UiO-66 (Zr_6 $O_4(OH)_4(BDC)_6$; BDC = benzene 1,4-dicarboxylic acid), a Zr-based MOF, were investigated using various molecular models and IGC methods [218]. The role of zeolitic imidazolate framework (ZIF-8) integrated into a polymer matrix in its monolithic form was examined using IGC. Thermodynamic properties of neat monoliths of butyl methacrylate-co-ethylene dimethacrylate and composite monoliths incorporating zeolitic imidazolate framework-8 with butyl methacrylate-co-ethylene dimethacrylate were studied under infinite dilution, 1 MPa column pressure, and different column temperatures [219]. Table 3 presents the characteristics of metal-organic frameworks and their composites determined using IGC.

4.8. Computer vision and image processing tools

4.8.1. Intricate visual traits

The use of image filtering techniques significantly enhances the quality of SEM images of the specimen's region of interest (ROI), particularly around the edges, which reveals the structural characteristics of the compound in each area. Additionally, edge feature extraction algorithms like Canny edge detection are employed to extract high-dimensional information about the compound from a visual perspective. To facilitate a comprehensive visual inspection of the compound's characteristics, intra-space contrast enhancement is applied, which brings out the intricate visual features. The results of the investigation into the intricate visual traits of Poly (Vinylidene Chloride-*Co*-Acrylonitrile) (P(VDC-*co*-AN)) and the polymer resin amberlite XAD-7 are presented below in Fig. 10, using a unified approach.

4.8.2. Surface roughness

An adaptive histogram equalization algorithm is utilized in image processing to preserve the proper spatial distribution [220]. By obtaining the difference image of the histogram equalized image, an adequate pixel distribution is achieved while retaining the roughness element. For surface roughness visualization in 3D and to obtain relevant roughness parameters for scientific experiments, computational tools such as Image J [110] and SPIP [221] are employed on the specimen. The outcomes of the customized pipeline for estimating and visualizing surface roughness in the polymer resin amberlite XAD-7 and Poly

Table 3
IGC physicochemical properties of Metal Organic Frame works (MOFs) and their composites.

Parameter	Compound	References
Dispersive Surface free energy	TAPPy-PDA COFs; MIL–100(Fe); Zr-based MOF; UiO-66 (Zr_6 $O_4(OH)_4$ $(BDC)_6$; BDC = benzene 1,4-dicarboxylic acid); ultrasmall Ti MOF (NH2-MIL-125(Ti))	[212–215]
Enthalpy of Adsorption	TAPPy-PDA COFs; MIL–100(Fe); Zr-based MOF; UiO-66 (Zr_6 $O_4(OH)_4$ $(BDC)_6$; BDC = benzene 1,4-dicarboxylic acid); ultrasmall Ti MOF (NH2-MIL-125(Ti))	[212–215]
Entropy of Adsorption	TAPPy-PDA COFs; MIL–100(Fe); Zr-based MOF; UiO-66 (Zr_6 $O_4(OH)_4$ $(BDC)_6$; BDC = benzene 1,4-dicarboxylic acid); ultrasmall Ti MOF (NH2-MIL-125(Ti))))	[212–215]
Acid Base Properties	TAPPy-PDA COFs; MIL–100(Fe); Zr-based MOF; UiO-66 (Zr_6 $O_4(OH)_4$ $(BDC)_6$; BDC = benzene 1,4-dicarboxylic acid); ultrasmall Ti MOF (NH2-MIL-125(Ti))	[212–215]

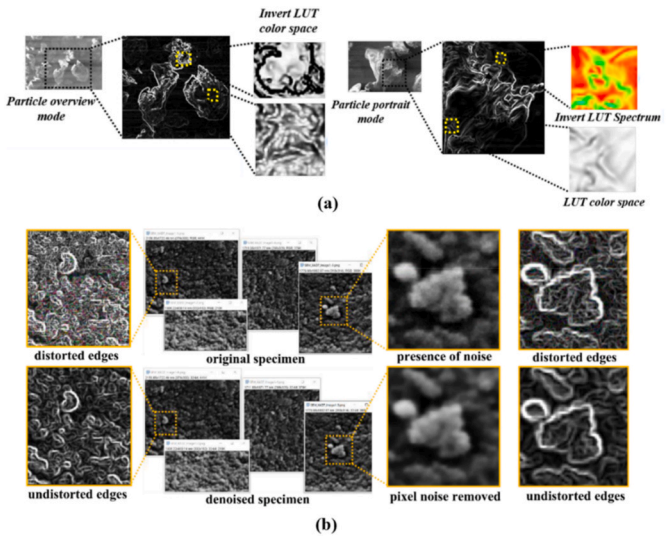

Fig. 10. Customized image analysis pipeline for: (a) exploring visual intricate patterns in polymer. (b) exploring visual intricate patterns in polymer resin.

(Vinylidene Chloride-*Co*-Acrylonitrile) (P(VDC-*co*-AN)) are presented below in Fig. 11, using a unified approach. These results provide valuable insights into the surface characteristics of the materials.

4.8.3. Particle distribution, porosity and dimensionality

The directionality analysis employs frequency-based Fourier components to reveal both low and high frequency components in the specimen, allowing for the estimation of local gradient orientation of individual particles. The information obtained from porosity and directionality will serve as metadata for future experiments, particularly in relation to the compound's absorption capability in specific directions. The outcomes of the Computer Vision and Image Processing (CVIP) methods used to estimate particle distribution, porosity, and directionality in the polymer resin amberlite XAD-7 and Poly (Vinylidene Chloride-*Co*-Acrylonitrile) (P(VDC-*co*-AN)) are presented below in Fig. 12, utilizing a comprehensive approach. These results provide valuable insights into the compound's structural characteristics and absorption behavior.

4.9. Artificial intelligence (AI) and machine learning (ML) tools

The usage of artificial intelligence and machine learning can be categorized as mostly the predictive analytics part of the IGC and related research studies. Meaning that, the IGC process and its results could be refactored using AI and ML tools for predicting certain parameters and relevant characteristics. There were several notable works in the IGC domain that were conducted with the assistance of AI/ML tools as the main elements of predicting outcomes of the research study. Table 4, states the notable works of AI and ML convergence in the field of IGC and other associated fields that utilize the IGC data.

4.9.1. Polymer characterization and material science

The co-existence of AI and ML tools with IGC data was explored in the polymer characterization aspect where the artificial neural networks are used to predict polymer properties based on IGC data, demonstrating greater accuracy and efficiency than traditional methods [222,223]. A diverse amount of machine learning techniques, including random forests and support vector machines, were used to analyze IGC data and identify material properties and interactions [224,225].

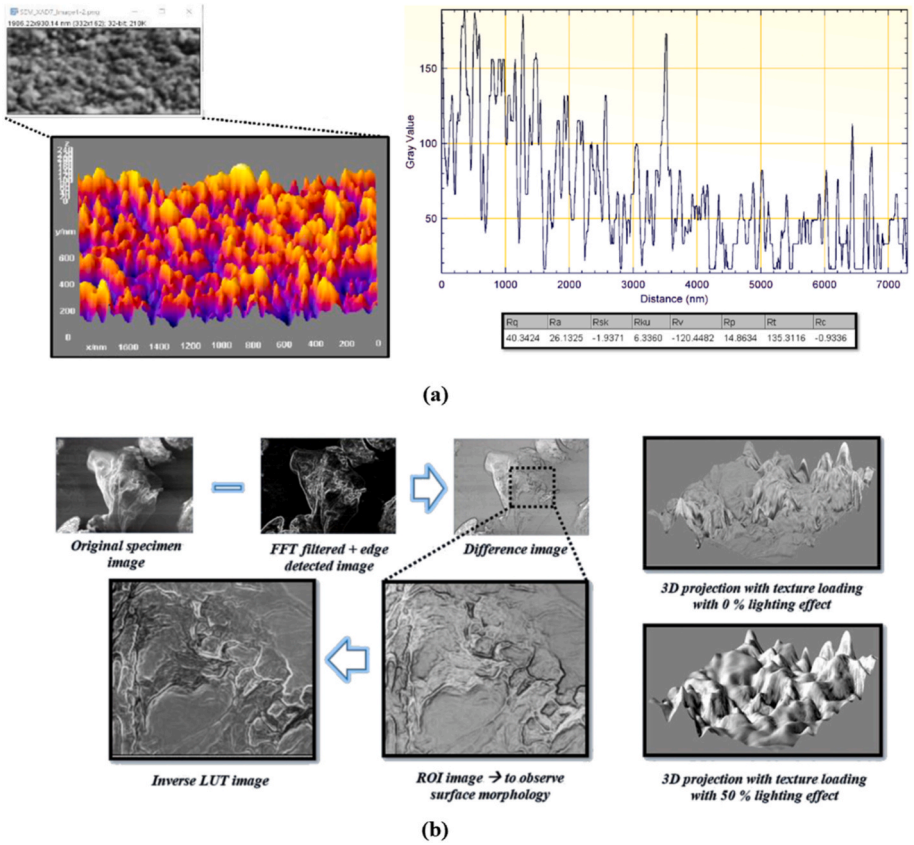

Fig. 11. Outcome of the customized image analysis pipeline for: (a) estimating roughness parameters of polymer resin. (b) Visualizing surface roughness of polymer.

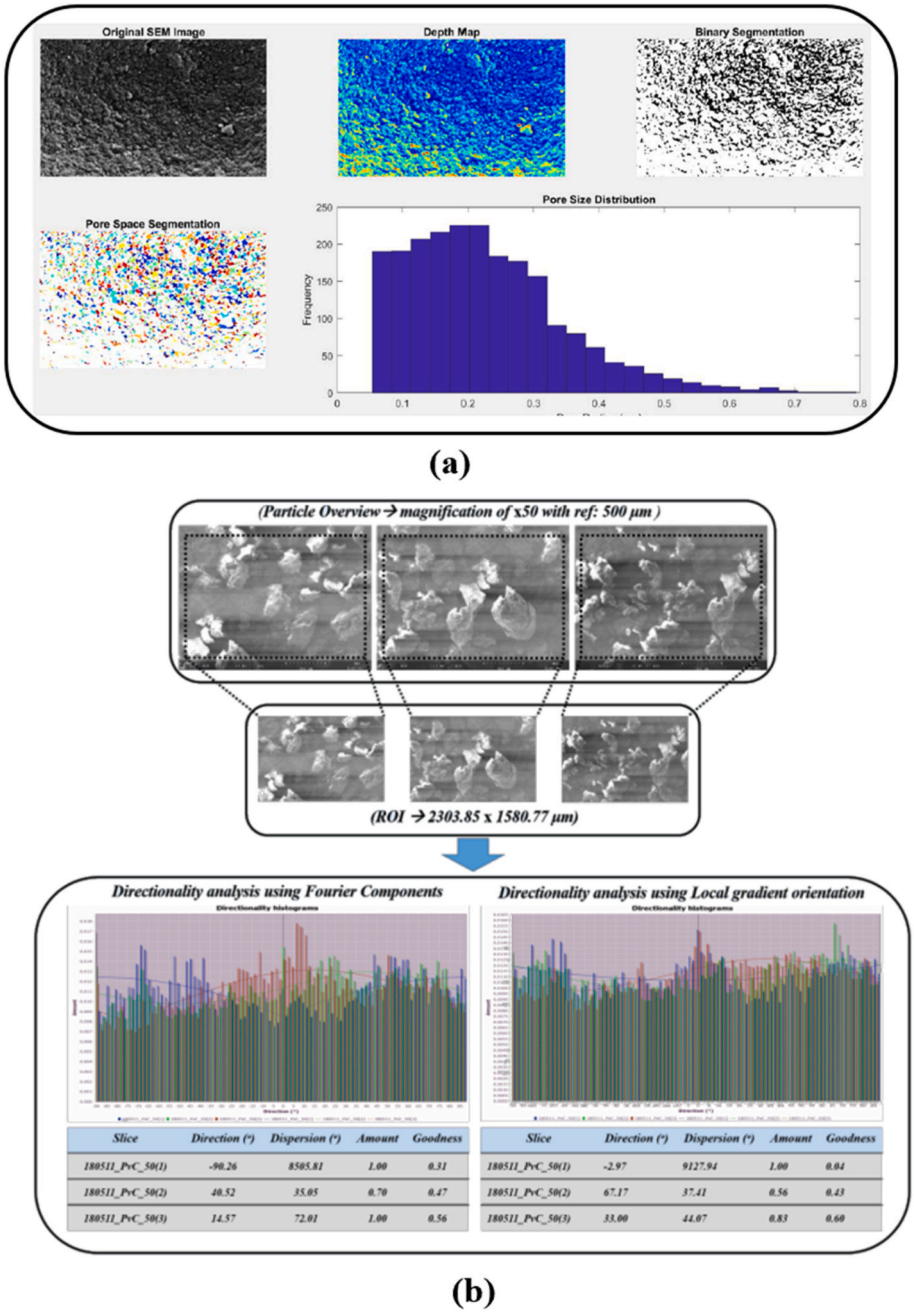

Fig. 12. Outcome of the CVIP pipeline for: (a) estimating porosity and particle distribution of polymer resin. (b) estimating directionality of polymer.

4.9.2. Surface science and solvent analysis

There were few studies that focused on the use of AI algorithms, including genetic algorithms and neural networks, to extract surface properties from IGC measurements, allowing for improved surface characterization [226,227]. Also, studies such as [228,229] used machine learning algorithms to accurately predict solubility parameters of solvents based on IGC data, thereby facilitating solvent selection.

4.9.3. Pharmaceutical analysis and separation science

The combination of an AI-based approach for characterizing pharmaceutical powders using IGC data, allowing for rapid evaluation of powder properties and formulation optimization was carried out by Refs. [230,231]. Furthermore, few studies utilized AI-based predictive models to optimize vapor phase separation of organic compounds in IGC, resulting in increased separation efficiency and selectivity [232, 233].

4.9.4. Surface energy and bitumen analysis

Machine learning methods, such as decision trees and neural networks were employed for estimating surface energy parameters from IGC measurements, providing accurate and efficient analysis [234]. AI techniques, such as fuzzy logic and genetic algorithms were used to analyze polymer-modified bitumen using IGC, allowing for a better understanding of polymer-bitumen interactions [235,236].

4.9.5. Adsorption analysis and gas separation

There were studies demonstrating the use of artificial neural networks to predict adsorption isotherms based on IGC data, thereby offering valuable insights into adsorption behavior and material performance [237,238]. Also, certain studies used AI optimization algorithms, such as genetic algorithms and particle swarm optimization, to improve the separation efficiency of gas separation columns in IGC [240,241].

Table 4
Various research studies employing AI and ML tools on IGC data in diverse scenarios.

Technology used	Fields of convergence	Research scenario of using AI/ML tools with IGC data	Relevant studies
Artificial intelligence	Polymer Characterization	utilized artificial neural networks to predict polymer properties based on IGC data, demonstrating greater accuracy and efficiency than traditional methods.	[222] [223]
Machine learning	Material Science	investigated various machine learning techniques, including random forests and support vector machines, to analyze IGC data and identify material properties and interactions.	[224] [225]
Artificial intelligence	Surface Science	use of AI algorithms, including genetic algorithms and neural networks, to extract surface properties from IGC measurements, allowing for rapid characterization.	[226] l [227]
Machine learning	Solvent Analysis	used machine learning algorithms to accurately predict solubility parameters of solvents based on IGC data, thereby facilitating solvent selection.	[228] [229]
Artificial intelligence	Separation Science	utilized AI-based predictive models to optimize vapor phase separation of organic compounds in IGC, resulting in increased separation efficiency and selectivity.	[230] [231]
Artificial intelligence	Pharmaceutical Analysis	AI-based approach for characterizing pharmaceutical powders using IGC data, allowing for rapid evaluation of powder properties and formulation optimization.	[232] [233]
Machine learning	Surface Energy Analysis	examined machine learning methods, such as decision trees and neural networks, for estimating surface energy parameters from IGC measurements, providing accurate and efficient analysis.	[234]
Artificial intelligence	Bitumen Analysis	used AI techniques, such as fuzzy logic and genetic algorithms, to analyze polymer-modified bitumen using IGC, allowing for a better understanding of polymer-bitumen interactions.	[235] [236]
Artificial intelligence	Adsorption Analysis	use of artificial neural networks to predict adsorption isotherms based on IGC data, thereby offering valuable insights into adsorption behavior and material performance.	[237] [238]
Artificial intelligence	Gas Separation	used AI optimization algorithms, such as genetic algorithms and particle swarm optimization, to improve the separation efficiency of gas separation columns in IGC.	[239] [240]
Artificial intelligence	Fiber Analysis	investigated AI approaches, such as machine learning and pattern recognition, for evaluating surface properties of fibrous materials through IGC analysis, thereby facilitating material selection and development.	[241] [242]
Machine learning	Solvent Classification	employed machine learning-based classification model for organic solvents using IGC data, allowing for rapid screening and selection of organic solvents for a variety of applications	[243]
Artificial intelligence	Drug Formulation	combined IGC with AI techniques, such as clustering and classification algorithms, to investigate drug-excipient compatibility, thereby providing valuable insights for formulation development	[244]
Machine learning	Polymer Blends	used machine learning algorithms to predict polymer blend miscibility based on IGC data, enabling efficient screening of blend compositions to identify those with the desired properties	[245]

4.9.6. Fiber analysis and solvent classification

A few studies investigated AI approaches, such as machine learning and pattern recognition, for evaluating surface properties of fibrous materials through IGC analysis, thereby facilitating material selection and development [242,243]. Machine learning-based classification model for organic solvents using IGC data was also a method that facilitated rapid screening and selection of organic solvents for a variety of applications [244].

4.9.7. Drug formulation and polymer blends

There were studies that combined IGC with AI techniques, such as clustering and classification algorithms, to investigate drug-excipient compatibility, thereby providing valuable insights for formulation development [280]. Furthermore, there were instances where machine learning algorithms were used to predict polymer blend miscibility based on IGC data, enabling efficient screening of blend compositions to identify those with the desired properties [245].

5. Perspective

The combination of these two technologies (IGC + AI) creates a novel platform for thorough material characterization and the development of enhanced procedures. Examples of the effectiveness of integrating such methods include thermal modeling for anionic surfactants, assessment of surface thermodynamic properties using reverse phase chromatography, and characterization of polymer surface thermodynamics. In the aforementioned areas, researchers have utilized artificial intelligence and machine learning technologies to improve the precision and effectiveness of material property forecasts using IGC data.

Although there have been positive results, there are still difficulties in combining IGC and AI. A major obstacle is in the intricate process of integrating data from chromatographic outputs with their corresponding visual characteristics, which are greatly influenced by the SEM/TEM apparatus. When there is a noisy measurement, the accuracy is compromised, which in turn affects the AI pipeline. Furthermore, the process of establishing uniform procedures and frameworks for interpreting data continues to be a difficult task at this point. Subsequent investigations should prioritize the enhancement of data fusion methodologies to effectively incorporate IGC and AI data pipeline. Furthermore, the development of machine learning algorithms specifically

designed for the analysis of multi-modal data will be of utmost importance. Standardizing techniques and creating benchmark datasets will make it easier to compare and replicate investigations.

The synergistic application of IGC with AI has significant practical implications, especially within the pharmaceutical and chemical sectors. Efficient and precise analysis of material properties, including surface energy, thermodynamic parameters, and compatibility assessments, will accelerate the formulation creation and optimization procedures. Moreover, the capacity to visually perceive surface characteristics improves comprehension of material behavior and performance, hence facilitating well-informed decision-making in the selection and development of materials.

6. Conclusions

Inverse gas chromatography (IGC) has emerged as a valuable and evolving technique in the field of materials science. The historical evolution of IGC, stemming from its origins in gas chromatography (GC), has positioned it as a versatile technique for investigating the physicochemical properties of materials. Over the past several decades, IGC has proven its efficacy in characterizing both the surface and bulk properties of various materials. Its adaptability, precision, and simplicity make it a valuable tool in analytical laboratories. Furthermore, the integration of IGC with artificial intelligence (AI) and computer vision and image processing (CVIP) techniques holds great promise. By combining IGC with AI and CVIP, researchers can gain a comprehensive understanding of the chemical and physical aspects of materials, particularly their surface characteristics. This convergence opens up new avenues for exploring the complexities of advanced materials and provides valuable insights into their behavior.

This review serves as a comprehensive overview of IGC's advancements and its potential convergence with AI and CVIP. The synergistic combination of IGC and CVIP offers exciting opportunities for advancing our understanding of advanced materials and their surface properties. By harnessing the power of IGC, AI, and CVIP, researchers can accelerate material discovery and development, leading to the design of innovative materials with tailored properties and enhanced performance. Additionally, the integration of IGC with AI and CVIP can contribute to the advancement of fundamental scientific understanding in areas such as interfacial phenomena, adsorption kinetics, and surface chemistry. By utilizing machine learning algorithms and advanced image analysis techniques, researchers can uncover intricate relationships between material structure, surface properties, and performance. This knowledge can be leveraged to develop new theoretical models, validate existing theories, and refine our understanding of complex material systems.

In summary, the convergence of IGC, AI, and CVIP holds great promise for pushing the frontiers of edge-cutting areas in materials science. From the design of advanced functional materials to quality control in industries and fundamental scientific investigations, the integration of these techniques can lead to transformative advancements. By embracing this multidisciplinary approach, researchers can unlock new opportunities for innovation, discovery, and optimization in materials science and related fields.

Additionally, the convergence of IGC, AI, and CVIP holds great promise for pushing the frontiers of edge-cutting areas in materials science. From the design of advanced functional materials to quality control in industries and fundamental scientific investigations, the integration of these techniques can lead to transformative advancements. By embracing this multidisciplinary approach, researchers can unlock new opportunities for innovation, discovery, and optimization in materials science and related fields. This knowledge can be leveraged to develop new theoretical models, validate existing theories, and refine our understanding of complex material systems.

Compliance with ethics gemailuidelines

All authors declared that there is no conflict of interest.

CRediT authorship contribution statement

Praveen Kumar Basivi: Writing – original draft, Visualization, Validation, Software, Resources, Methodology, Investigation, Formal analysis, Data curation, Conceptualization. **Tayssir Hamieh:** Validation, Methodology, Formal analysis, Conceptualization. **Vijay Kakani:** Writing – original draft, Methodology, Formal analysis, Data curation. **Visweswara Rao Pasupuleti:** Resources, Methodology, Data curation. **G. Sasikala:** Formal analysis. **Sung Min Heo:** Software, Formal analysis. **Kedhareswara Sairam Pasupuleti:** Validation. **Moon-Deock Kim:** Visualization, Resources. **Venkata Subbaiah Munagapati:** Formal analysis. **Nadavala Siva Kumar:** Validation, Formal analysis. **Jet-Chau Wen:** Methodology, Formal analysis. **Chang Woo Kim:** Writing – review & editing, Visualization, Supervision, Project administration, Funding acquisition, Formal analysis, Data curation.

Declaration of competing interest

The authors declare no competing interests.

Data availability

Data will be made available on request.

Acknowledgements

This research was supported by Basic Science Research Program through the National Research Foundation of Korea (NRF) funded by the Ministry of Education (2020R1I1A3072987).

References

[1] Nobel Laureates in Chemistry, 1901-1992, Wiley VCH, 1993.
[2] K. Shcherbakova, Y.I. Yashin, V. Andrej, Kiselev's contributions to the science of ad sorption, molecular interaction and chromatography, Pure Appl. Chem. 61 (1989) 1829–1834.
[3] A.V. Kiselev, Y.I. Yashin, J. Bradley, Gas-Adsorption Chromatography, Plenum Press, New York, 1969.
[4] J.R. Conder, C.L. Young, Physicochemical Measurements by Gas Chromatography, John Wiley & Sons, New York, 1979.
[5] R.J. Laub, R.L. Pescock, Physicochemical Applications of Gas Chromatography, Wiley, New York, 1978.
[6] J.R. Conder, C.L. Young, Physicochemical Measurement by Gas Chromatography, Wiley, New York, 1979.
[7] D. Butler, D.R. Williams, Particulate characterization: inverse gas chromatography, in: I.D. Wilson (Ed.), Encyclopedia of Separation Science, Elsevier Science Ltd., 2000, pp. 3609–3614.
[8] A. Lavoie, J. Guillet, Estimation of glass transition on temperatures from gas chromatographic studies on polymers, Macromolecules 2 (1969) 443–446.
[9] J.R. Conder, D.C. Locke, J.H. Purnell, Concurrent solution and adsorption phenomena in chromatography. I, J. Phys. Chem. 73 (1969) 708–712.
[10] J. Conder, J. Purnell, Gas chromatography at finite concentrations. Part 1. —effect of gas imperfection on calculation of the activity coefficient in solution from experi- mental data, Trans. Faraday Soc. 64 (1968) 1505–1512.
[11] J. Conder, J. Purnell, Gas chromatography at finite concentrations. Part 2. —a gener- alised retention theory, Trans. Faraday Soc. 64 (1968) 3100–3111.
[12] J. Conder, J. Purnell, Gas chromatography at finite concentrations. Part 3. —theory of frontal and elution techniques of thermodynamic measurement, Trans. Faraday Soc. 65 (1969) 824–838.
[13] J. Conder, J. Purnell, Gas chromatography at finite concentrations. Part 4. —experi- mental evaluation of methods for thermodynamic study of solutions, Trans. Faraday Soc. 65 (1969) 839–848.
[14] O. Smidsrød, J. Guillet, Study of polymer-solute interactions by gas chromatography, Macromolecules 2 (1969) 272–277.
[15] T. Davis, J. Petersen, W. Haines, Inverse gas-liquid chromatography. A new approach for studying petroleum asphalts, Anal. Chem. 38 (1966) 241–243.
[16] J.E. Guillet, Molecular probes in the study of polymer structure, J. Macromol. Sci., Chem. (1970) 1669–1674.
[17] R.A. Meyers (Ed.), Encyclopedia of Analytical Chemistry: Cpplications, Theory and Instrumentation, Wiley, Chichester, 2000.
[18] R. Vilcu, M. Leca, Polymer Thermodynamics by Gas, Elsevier, Amsterdam, 1990.

[19] A.J. Ashworth, D.M. Hooker, Mixed solvents in gas-liquid chromatography: activity coefficients for benzene, cyclohexane, pentane and heptane in squalane-dinonyl phthalate mixtures at 303 °K, J. Chromatogr., A 174 (1979) 307–313.
[20] M.W.P. Harbison, R.J. Laub, D.E. Martire, J.H. Purnell, P.S. Williams, Solute infinite-dilution partition coefficients with mixtures of squalane and dinonyl phthalate solvents at 30.0°C, J. Phys. Chem. 83 (10) (1979) 1262–1268.
[21] L. Bonifaci, G.P. Ravanetti, Measurement of infinite dilution diffusion coefficients of ϵ-caprolactam in nylon 6 at elevated temperatures by inverse gas chromatography, J. Chromatogr., A 607 (1992) 145–149.
[22] D.F. Steele, R.C. Moreton, J.N. Staniforth, P.M. Young, M.J. Tobyn, S. Edge, Surface energy of microcrystalline cellulose determined by capillary Intrusion and inverse gas chromatography, AAPS J. 3 (2008) 494–503.
[23] K.L. Mittal, H.R. Anderson, Acid-Base Interactions Relevance to Adhesion Science and Technology, VSP, Utrecht the Netherlands, 1991.
[24] T.C. Ward, D.R. Lloyd, H.P. Schreiber (Eds.), Inverse Gas Chromatography, Characterization of Polymers and Other Materials, ACS, Washington; DC, 1989.
[25] C.R. Schaefer, M.E.F. De Ruiz Holgado, E.L. Arancibia, Sucrose derivative surfactants studied by inverse gas chromatography, J. Colloid Interface Sci. 239 (2001) 222–225.
[26] A. Dabrowski, V.A. Tertykh, Adsorption on new and modified inorganic sorbents, in: Studies in Surface Science and Catalysis vol. 99, Elsevier, Amsterdam, 1996, 9780080526027.
[27] B.C. Hancock, P. York, R.C. Rowe, The use of solubility parameters in pharmaceutical dosage form design, J. Pharmaceut. Sci. 148 (1997) 1–21.
[28] C. Perruchot, M.M. Chehimi, M. Delamar, S.F. Lascelles, S.P. Armes, A physicochemical study of poly pyrrole-silica nanocomposites by inverse gas chromatography, J. Colloid Interface Sci. 193 (1997) 190–199.
[29] K. Adamska, A. Voelkel, Inverse gas chromatographic determination of solubility parameters of excipients, International Journal of Pharmaceutical 304 (2005) 11–17.
[30] F. Gritti, G. Félix, M.F. Achard, F. Hardouin, Investigation of the nematic–isotropic transition of a liquid crystalline polymer and determination of molecular diffusion coefficients using gas chromatography, J. Chromatogr., A 893 (2000) 359–366.
[31] M.D. Ticehurst, P. York, R.C. Rowe, S.K. Dwivedi, Characterization of the surface properties of α-lactose monohydrate with inverse gas chromatography, used to detect batch variation, Int. J. Pharm. 141 (1996) 93–99.
[32] Z.Y. Al-Saigh, Review: inverse gas chromatography for the characterization of polymer blends, Int J Polym Sci. 3 (1997) 249–291.
[33] J.M.R.C.A. Santos, J.T. Guthrie, Analysis of interactions in multicomponent polymeric systems: the key-role of inverse gas chromatography, Mater. Sci. Eng. R Rep. 50 (2005) 79–107.
[34] C.M. Hansen, Hansen solubility parameters, in: A User's Handbook, CRC Press, Boca Raton, FL, 2000.
[35] A.N. Nastasović, A.E. Onjia, Determination of glass temperature of polymers by inverse gas chromatography, J. Chromatogr., A 1195 (2008) 1–15.
[36] A. Shakhboz, S. Miraliev, V. Kakani, H. Kim, Joint multiclass object detection and semantic segmentation for autonomous driving, IEEE Access 11 (2023) 37637–37649.
[37] S. Tehreem, V. Kakani, X. Cui, H. Kim, Exploring optimized spiking neural network architectures for classification tasks on embedded platforms, Sensors 21 (9) (2021) 3240.
[38] V. Kakani, S. Lee, X. Cui, H. Kim, Performance analysis of spiking neural network using temporal spike-based backpropagation on field programmable gate array (FPGA) platform, in: 2022 IEEE Region 10 Symposium (TENSYMP), IEEE, 2022, pp. 1–6.
[39] M. Shokhrukh, S. Abdigapporov, V. Kakani, H. Kim, Real-time memory efficient multitask learning model for autonomous driving, IEEE Transactions on Intelligent Vehicles 8 (2023) 1–12.
[40] G. Akash, V. Kakani, H. Kim, SSRT: a sequential skeleton RGB transformer to recognize fine-grained human-object interactions and action recognition, IEEE Access 4 (2023) 1–19.
[41] J. Sardor, A. Ghimire, J. Alikhanov, V. Kakani, H. Kim, "Exploring human pose estimation and the usage of synthetic data for elderly fall detection in real-world surveillance, IEEE Access 10 (2022) 94249–94261.
[42] V. Kakani, H. Kim, Adaptive self-calibration of fisheye and wide-angle cameras, IEEE 10 (2019) 976–981.
[43] A.T. James, A.J.P. Martin, Gas-liquid partition chromatography: the separation and micro-estimation of volatile fatty acids from formic acid to dodecanoic acid, J. Biol. Chem. 50 (1952) 679–690.
[44] E. Papirer, H. Balard, E. Brendle, J. Lignieres, Inverse gas chromatography investigation of the surface characteristics of stainless steel tubing, J. Adhes. Sci. Technol. 10 (1996) 1401–1411.
[45] M.N. Belgacem, A.E. Gandini, Pefferkorn, in: Interfacial Phenomena in Chromatography, Marcel Dekker, New York, 1999, p. 41.
[46] E. Papirier, H. Balard, A. Vidal, Inverse gas chromatography: a valuable method for the surface characterization of fillers for polymers (glass fibers and silicas), Eur. Polym. J. 24 (1998) 783–790.
[47] J.M.R.C.A. Santos, M.H. Gil, A. Portugal, J.T. Guthrie, Characterisation of the surface of a cellulosic multi-purpose office paper by inverse gas chromatography, Cellulose 8 (2001) 217–224.
[48] C.S. Flour, E. Papirer, Gas solid chromatography: a quick method of estimating surface free energy variations induced by the treatment of short glass fibers, J. Colloid Interface Sci. 91 (1983) 69–75.
[49] F.M. Fowkes, Quantitative characterization of the acid-base properties of solvents, polymers, and inorganic surfaces, J. Adhes. Sci. Technol. 4 (1990) 669–691.
[50] M. Nardin, J. Schultz, Relationship between fiber-matrix adhesion and the interfacial shear strength in polymer-based composites, Compos. Interfac. 1 (1993) 177–192.
[51] B. Bilinski, L. Holysz, Some theoretical and experimental limitations in the determination of surface free energy of siliceous solids, Powder Technol. 102 (1999) 120–126.
[52] J. Schultz, L. Lavielle, Lloyd, D.R. Ward, T.C.H.P. Schreiber, (Eds.) Inverse Gas Chromatography. Characterization of Polymers and Other Materials. A.C.S, Washington. (1989) p. 185.
[53] D.P. Kamdem, S.K. Bose, P. Luner, Inverse gas chromatography characterization of birch wood meal, Langmuir 9 (1993) 3039–3044.
[54] G.M. Dorris, D.G. Gray, Adsorption of n-alkanes at zero surface coverage on cellulose paper and wood fibers, J. Colloid Interface Sci. 77 (1980) 353–362.
[55] G. Garnier, W.G. Glasser, Measurement of the surface free energy of amorphous cellulose by alkane adsorption: a critical evaluation of inverse gas chromatography (IGC), J. Adhes. 46 (1994) 165–180.
[56] A. Voelkel, K. Batko, K. Adamska, B. Strzemiecka, Determination of hansen solubility parameters by means of gas–solid inverse gas chromatography, Adsorpt. Sci. Technol. 26 (2008) 93–102.
[57] B. Shi, Y. Wang, L. Jia, Comparison of Dorris–Gray and Schultz methods for the calculation of surface dispersive free energy by inverse gas chromatography, J. Chromatogr., A 1218 (2011) 860–862.
[58] P.I. Mukhopadhyay, H.P. Schreiber, Aspects of acid-base interactions and use of inverse gas chromatography, Colloids Surf. A Physicochem. Eng. Asp. 100 (1995) 47–71.
[59] D.T. Sawyer, D.J. Brookman, Thermodynamically based gas chromatographic retention index for organic molecules using salt-modified aluminas and porous silica beads, J. Anal. Chem. 40 (1968) 1847–1853.
[60] J.B. Donnet, R.Y. Qin, M.J. Wang, A new approach for estimating the molecular areas of linear hydrocarbons and their derivatives, J. Colloid Interface Sci. 153 (1992) 572–577.
[61] E. Brendlé, E. Papirer, H. Balard, J. Dentzer, Variation of the surface properties of nickel o tide upon heat treatment evidenced by temperature programmed desorption and inverse gas chromatography studies, J. Mater. Sci. 35 (2000) 3573–3577.
[62] X. Kong, M. Dulce, L.V. Silveria, L. Zaho, P. Choi, A pseudo equation-of-state approach for the estimation of solubility parameters of polyethylene by inverse gas chromatography, Macromolecules 35 (2002) 8586–8590.
[63] T. Hamieh, M. Rezzaki, J. Schultz, Determination des Transitions Vitreuses et Locales de PMMA/Al2O3 Par des Methodes Thermiques et Chromatographiques, J. Therm. Anal. 51 (1998) 793–804.
[64] V. Gutmann, Donor–Acceptor Approach to Molecular Interactions, Plenum Press, N.Y, 1978.
[65] F.L. Riddle, F.M. Fowkes, Spectral shifts in acid-base chemistry. 1. van der Waals contributions to acceptor numbers, J. Am. Chem. Soc. 112 (1990) 3259–3264.
[66] E. Fekete, J. Moczo, B. Pukanszky, Determination of the surface characteristics of particulate fillers by inverse gas chromatography at infinite dilution: a critical approach, J. Colloid Interface Sci. 269 (2004) 143–152.
[67] H. Grajek, Rediscovering the problem of interpretation of chromatographically determined enthalpy and entropy of adsorption of different adsorbates on carbon materials: critical appraisal of literature data, J. Chromatogr., A 1145 (2007) 1–50.
[68] H. Chtourou, B. Riedl, B.V. Kokta, Surface characterizations of modified polyethylene pulp and wood pulps fibers using XPS and inverse gas chromatography, J. Adhes. Sci. Technol. 9 (1995) 551–574.
[69] Berg, J.C.D.A. Dillard, A.V. Pocius, M. Chaundhury (Eds.), Adhesion Science and Engineering, the Mechanics of Adhesion/Surfaces, Chemistry Applications, vol. 2, Elseivier, Amsterdam, 2002 (Chapter 1).
[70] E. Chibowski, R. Perea- Carpio, A novel method for surface free-energy determination of powdered solids, J. Colloid Interface Sci. 240 (2001) 473–479.
[71] T. Hamieh, J. Schultz, New approach to characterise physicochemical properties of solid substrates by inverse gas chromatography at infinite dilution. I. Some new methods to determine the surface areas of some molecules adsorbed on solid surfaces, J. Chromatogr., A 969 (2002) 17–36.
[72] T. Hamieh, M. Rageul-Lescouet, M. Nardin, H. Haidara, J. Schultz, Study of acid-base interactions between some metallic oxides and model organic molecules, Colloids Surf. A Physicochem. Eng. Asp. 125 (1997) 155–161.
[73] T. Hamieh, A.A. Ahmad, T. Roques-Carmes, J. Toufaily, New approach to determine the surface and interface thermodynamic properties of H-β-zeolite/rhodium catalysts by inverse gas chromatography at infinite dilution, Sci. Rep. 1 (2020) 1–27.
[74] A. Voelkel, B. Strzemiecka, K. Adamska, K. Milczewska, Inverse gas chromatography as a source of physiochemical data, J. Chromatogr., A 1216 (2008) 1551–1566.
[75] B.C. Hancock, P. York, C. Rowe, The use of solubility parameters in pharmaceutical dosage form design, Int. J. Pharm. 148 (1997) 1–21.
[76] H. Balard, E. Brendle, C. Vergelati, in: 3rd International Wood and Natural Fiber Composites Symposium, 2000.
[77] H. Wang, B. Li, B. Shi, Preparation and surface acid-base properties of porous cellulose, Bioresources 3 (1) (2008) 3–12.
[78] R.H. Mills, D.J. Gardner, R. Wimmer, Inverse gas chromatography for determining the dispersive surface free energy and acid–base interactions of sheet

molding compound—Part II 14 Ligno-cellulosic fiber types for possible composite reinforcement, J. Appl. Polym. Sci. 110 (2008) 3880–3888.
[79] M. Perez, M.C. A-Almazan, L. M-Linan, Evaluation of the dispersive component of the surface energy of active carbons as determined by inverse gas chromatography at zero surface coverage, J. Chromatogr., A 1214 (2008) 121–127.
[80] C. Perruchot, M.M. Chehimi, M.-J. Vaulay, K. Benzarti, Characterisation of the surface thermodynamic properties of cement components by inverse gas chromatography at infinite dilution, Cement Concr. Res. 36 (2006) 305–319.
[81] Y.C. Yang, B.G. Kim, S.B. Jeong, P.R. Yoon, Examination of acid–base properties of alumina treated with silane coupling agents, by using inverse gas chromatography, Powder Technol. 188 (2009) 29–33.
[82] S. Lazarevic, Z. Radovanovic, D.N. Veljovic, A. Onjia, D.T. Janackovic, R. Petrovic, Characterization of sepiolite by inverse gas chromatography at infinite and finite surface coverage, Appl. Clay Sci. 43 (2009) 41–48.
[83] B. Sasa, P. Odon, S. Stane, K. Julijana, Analysis of surface properties of cellulose ethers and drug release from their matrix tablets, Eur. J. Pharmaceut. Sci. 27 (2006) 375–383.
[84] P.M. Kosaka, Y. Kawano, D.F.S. Petri, De wetting and surface properties of ultrathin films of cellulose esters, J. Colloid Interface Sci. 316 (2007) 671–677.
[85] L. Patterson, A.P. Mathew, K. Oksman, Dispersion and properties of cellulose nanowhiskers and layered silicates in cellulose acetate butyrate nanocomposites, J. Appl. Polym. Sci. 112 (2009) 2001–2009.
[86] R. Wu, D. Que, Z.Y. Al-Saigh, Surface and thermodynamic characterization of conducting polymers by inverse gas chromatography: II. Polyaniline and its blend, J. Chromatogr., A 1146 (2007) 93–102.
[87] E. Papirier, H. Balard, E. Pefferkorn (Eds.), Interfacial Phenomena in Chromatograpahy, Marcel Dekker, New York, 1999, p. 145.
[88] M. Nardin, J. Schultz, G. Akovali (Eds.), The Interfacial Interactions in Polymer Composites, Kluwer Academic Publishers, The Netherlands, 1993, p. 81.
[89] C. Sun, J.C. Berg, A review of the different techniques for solid surface acid–base characterization, Adv. Colloid Interface Sci. 105 (2003) 151–175.
[90] P.H. Rousset, P. Sellappan, P. Daoud, Effect of emulsifiers on surface properties of sucrose by inverse gas chromatography, J. Chromatogr., A 969 (2002) 7–101.
[91] H. Balard, D. Maafa, A. Santini, J.B. Donnet, Study by inverse gas chromatography of the surface properties of milled graphites, J. Chromatogr., A 1198 (2008) 173–180.
[92] B. Shi, S. Zhao, L. Jia, L. Wang, Surface characterization of chitin by inverse gas chromatography, Carbohydr. Polym. 67 (2007) 98–402.
[93] X. Zhang, D. Yang, P. Xu, C. Wang, Q. Du, Characterizing the surface properties of carbon nanotubes by inverse gas chromatography, J. Mater. Sci. 42 (2007) 7069–7075.
[94] J. Zhang, D.Y. Kwok, Calculation of Solid−Liquid work of adhesion patterns from combining rules for intermolecular potentials, J. Phys. Chem. B 106 (2002) 12594–12599.
[95] S. Peterlin, O. Planinsek, I. Mountinho, P. Ferreira, D. Dolenc, Inverse gas chromatography analysis of spruce fibers with different lignin content, Cellulose 17 (2010) 1095–1102.
[96] T. Hamieh, M.B. Fadlallah, J. Schultz, New approach to characterize physicochemical properties of solid substrates by inverse gas chromatography at infinite dilution: III. Determination of the acid–base properties of some solid substrates (polymers, oxides and carbon fibres): a new model, J. Chromatogr. A 969 (2002) 37–47.
[97] T. Hamieh, J. Schultz, New approach to characterize physicochemical properties of solid substrates by inverse gas chromatography at infinite dilution. II. Study of the transition temperatures of poly (methyl methacrylate) at various tacticities and of poly (methyl methacrylate) adsorbed on alumina and silica, J. Chromatogr. A 969 (1–2) (2002) 27–36.
[98] T. Hamieh, Study of the temperature effect on the surface area of model organic molecules, the dispersive surface energy and the surface properties of solids by inverse gas chromatography, J. Chromatogr., A 1627 (2020) 461372.
[99] P.K. Basivi, V. Kakani, T. Hamieh, S.M. Heo, V.R. Pasupuleti, C.W. Kim, Thermal modeling for anionic surfactant using Inverse gas chromatography and image processing techniques, J. Mol. Liq. 383 (2023) 122072.
[100] T. Hamieh, New progress on London dispersive energy, polar surface interactions and Lewis's acid-base properties of solid surfaces, Preprints. (2024) 2024010638.
[101] K. Vijay, V.H. Nguyen, B.P. Kumar, H. Kim, V.R. Pasupuleti, A critical review on computer vision and artificial intelligence in food industry, J. Agri. Food. Res. 2 (2020) 100033.
[102] K. Vijay, X. Cui, M. Ma, H. Kim, Vision-based tactile sensor mechanism for the estimation of contact position and force distribution using deep learning, Sensors 21 (5) (2021) 1920.
[103] K. Vijay, H. Kim, M. Kumbham, D. Park, C.B. Jin, V.H. Nguyen, Feasible self-calibration of larger field-of-view (FOV) camera sensors for the advanced driver-assistance system (ADAS), Sensors 19 (15) (2019) 3369.
[104] V. Kakani, H. Kim, J. Lee, C. Ryu, M. Kumbham, Automatic distortion rectification of wide-angle images using outlier refinement for streamlining vision tasks, Sensors 20 (3) (2020) 894.
[105] V. Kakani, H. Kim, B.P. Kumar, V.P. Rao, Surface thermo-dynamic characterization of poly (vinylidene chloride-co-acrylonitrile) (P (VDC-co-AN)) using inverse-gas chromatography and investigation of visual traits using computer vision image processing algorithms, Polymers 12 (8) (2020) 1631.
[106] B.P. Kumar, et al., Surface thermodynamic properties by reverse phase chromatography and visual traits using computer vision techniques on Amberlite XAD-7 acrylic-ester-resin, Polym. Adv. Technol. 33 (2022) 3572–3582.
[107] E. Cuevas, B. Héctor, L. Alberto, Anisotropic diffusion filtering through multi-objective optimization, Math. Comput. Simulat. 181 (2021) 410–429.
[108] M.G. Forero, et al., Comparative analysis of smoothing filters in confocal microscopy images, in: Applications of Digital Image Processing XLII, California, United States, Sep 6, 2019.
[109] K.R. Rao, D.N. Kim, J.H. Jae, Fast Fourier Transform: Algorithms and Applications, vol. 32, Springer, Dordrecht, 2010.
[110] C.A. Schneider, W.S. Rasband, K.W. Eliceiri, NIH Image to ImageJ: 25 years of image analysis, Nat. Methods 9 (2012) 671–675.
[111] Y. Lin, et al., Automatic cell counting for phase-contrast microscopic images based on a combination of Otsu and watershed segmentation method, Microsc. Res. Tech. 85 (1) (2022) 169–180.
[112] A. Rabbani, S. Salehi, Dynamic modeling of the formation damage and mud cake deposition using filtration theories coupled with SEM image processing, J. Nat. Gas Sci. Eng. 42 (2017) 157–168.
[113] M. Castellano, L. Falqui, G. Costa, A. Turturro, B. Valenti, G. Castello, Investigation on elastomer–silica interactions by inverse gas chromatography and image analysis aided transmission electron microscopy, J. Macromol. Sci., Part B 41 (3) (2002) 451–471.
[114] K. Sven, S.N. Krylov, Image processing and analysis system for development and use of free flow electrophoresis chips, Lab Chip 17 (2) (2017) 256–266.
[115] M. Kosmas, D. Gavril, Optimization of a microcontroller for the simultaneous logging of temperature and reversed-flow inverse gas chromatography measurements, Instrum. Sci. Technol. 46 (2) (2018) 222–244.
[116] A. Voelkel, K. Adamska, B. Strzemiecka, K. Batko, Determination of Hansen solubility parameters of solid materials by inverse gas-solid chromatography, Acta Chromatogr. 20 (2008) 1–14.
[117] P.E. Luner, Y. Zhang, Y.A. Abramov, M.T. Carvajal, Evaluation of milling method on the surface energetics of molecular crystals using inverse gas chromatography, Cryst. Growth Des. 12 (2012) 5271–5282.
[118] R. Menzel, A. Bismarck, M.S. Shaffer, Deconvolution of the structural and chemical surface properties of carbon nanotubes by inverse gas chromatography, Carbon 50 (2012) 3416–3421.
[119] T. Hamieh, New progress on London dispersive energy, polar surface interactions, and Lewis's acid–base properties of solid surfaces, Molecules 29 (2024) 949.
[120] A. Legras, A. Kondor, M.T. Heitzmann, R.W. Truss, Inverse gas chromatography for natural fiber characterisation: identification of the critical parameters to determine the Brunauer–Emmett–Teller specific surface area, J. Chromatogr., A 1425 (2015) 273–279.
[121] K. Yusuf, A. Yacine Badjah-Hadj-Ahmed, A. Aqel, T. Aouak, Z.A. Alothman, Zeolitic imidazolate framework-methacrylate composite monolith characterization by inverse gas chromatography, J. Chromatogr., A 1443 (2016) 233–240.
[122] T.V.M. Sreekanth, P.K. Basivi, P.C. Nagajyothi, G.R. Dillip, J. Shim, T.J. Ko, K. Yoo, Determination of surface properties and Gutmann's Lewis acidity–basicity parameters of thiourea and melamine polymerized graphitic carbon nitride sheets by inverse gas chromatography, J. Chromatogr., A 1580 (2018) 134–141.
[123] F. Eric, C. Joungmo, Y. Jihnhee, Z.Y. Al-Saigh, K. Joonyeong, Adsorption of hydrocarbons commonly found in gasoline residues on household materials studied by inverse gas chromatography, J. Chromatogr., A 1594 (2019) 149–159.
[124] S. Baoli, Problem in the molecular area of polar probe molecules used in inverse gas chromatography, J. Chromatogr., A 1601 (2019) 385–387.
[125] F. Bauer, R. Meyer, S. Czihal, M. Bertmer, U. Decker, S. Naumov, H. Uhlig, M. Steinhart, D. Enke, Functionalization of porous siliceous materials, Part 2: surface characterization by inverse gas chromatography, J. Chromatogr., A 1603 (2019) 297–310.
[126] K. Tamargo-Martínez, M.A. Montes-Morán, A. Martínez-Alonso, J.M.D. Tascón, Effect of non-oxidative plasma treatments on the surface properties of poly (*p* -phenylene terephthalamide) (PPTA) and poly (*p* -phenylene benzobisoxazole) (PBO) fibres as measured by inverse gas chromatography, J. Chromatogr., A 1634 (2020) 461655.
[127] F. Eric, C. Carleigh, Y. Jihnhee, A.S. Zeki, Y.K. Joonyeong, Investigation of sorption and diffusion of hydrocarbons into polydimethylsiloxane in the headspace-solid phase microextraction sampling process via inverse gas chromatography, J. Chromatogr., A 1639 (2021) 461894.
[128] B.P. Kumar, P.V. Rao, T. Hamieh, C.W. Kim, Comparative study of nitrogen doped multi walled carbon nanotubes grafted with carboxy methyl cellulose hybrid composite by inverse gas chromatography and its UV photo detectors application, J. Chromatogr., A 1670 (2022) 462997.
[129] S. Baoli, Inverse gas chromatography as a tool for screening materials: the relation between Lewis acid–base constants and triboelectric charge density of polymers, J. Chromatogr., A 1675 (2022) 463131.
[130] S.Y. Lee, J.H. Lee, Y.H. Kim, R.L. Mahajan, S.J. Park, Surface energetics of graphene oxide and reduced graphene oxide determined by inverse gas chromatographic technique at infinite dilution at room temperature, J. Colloid Interface Sci. 628 (2022) 758–768.
[131] A. Voelkel, B. Strzemiecka, K. Milczewska, Z. Okulus, Inverse gas chromatographic examination of polymer composites, Open Chem. 13 (2015) 893–900.
[132] E.L. Arancibia, P.C. Schulz, S.M. Bardavid, Interaction parameters of surfactant mixtures by inverse gas chromatography, Applications of Gas Chromatography. 31211 (2012) 17–40.
[133] Y. Yampolski, N. Belov, Investigation of polymers by inverse gas chromatography, Macromolecules (Washington, DC, U. S.) 48 (2015) 6751–6767.

[134] N.U. Rahman, M.K. Sarfraz, S. Mohsin, Characterization and quantification of pH sensitive polymers used in drug targeting by inverse-phase gas chromatography and dynamic vapour sorption techniques, Mater. Express. 6 (2016) 344–350.
[135] G.L. Klein, G. Pierre, M.N.B. Fontaine, M. Graber, Inverse gas chromatography with film cell unit : an attractive alternative method to characterize surface properties of thin films, J. Chromatogr. Sci. 53 (2015) 1233–1238.
[136] J. Zhang, S. Du, A. Kafi, B. Fox, J.L. Li, X.Y. Liu, R. Rajkhowa, X.G. Wang, Surface energy of silk fibroin and mechanical properties of silk cocoon composites, RSC Adv. 5 (2015) 1640.
[137] S. Ramanaiah, V. Karde, P. Venkateswarlu, C. Ghoroi, Effect of temperature on the surface free energy and acid–base properties of Gabapentin and Pregabalin drugs - a comparative study, RSC Adv. 5 (2015) 48712.
[138] Y. Xia, Z. Wu, B. Lu, T. Wang, J. Li, A modified UNIFAC-ZM model and phase equilibrium prediction of silicone polymers with ABE solution, RSC Adv. 6 (2016) 53643.
[139] M. Avgidou, M. Dimopoulou, A.R. Mackie, N.M. Rigby, C. Ritzoulis, C. Panayiotou, Physicochemical aspects of mucosa surface, RSC Adv. 6 (2016) 102634.
[140] E. Hadjittofis, G.G.Z. Zhang, J.Y.Y. Heng, Influence of sample preparation on IGC measurements: the cases of salinized glass wool and packing structure, RSC Adv. 7 (2017) 12194.
[141] G. Zhao, H. Ni, S. Ren, G. Fang, Correlation between solubility parameters and properties of alkali lignin/PVA composites, Polymers 10 (2018) 290.
[142] S. Chen, H. Yang, K. Huang, X. Ge, H. Yao, J. Tang, J. Ren, Y. Ma, Quantitative study on solubility parameters and related thermodynamic parameters of PVA with different alcoholysis degrees, Polymers 13 (21) (2021) 3778.
[143] A.Y. Kanatieva, D.A. Alentiev, V.E. Shiryaeva, A.A. Korolev, A.A. Kurganov, Impact of the polymer backbone structure on the separation properties of new stationary phases based on tricyclononenes, Polymers 14 (2022) 5120.
[144] A. Legras, M. Kondor, M.T. Alcock, M. Heitzmann, R.W. Truss, Inverse gas chromatography for natural fiber characterisation: dispersive and acid-base distribution profiles of the surface energy, Cellulose 24 (2017) 4691–4700.
[145] A.Ç. Adiguzel, B. Korkmaz, F. Çakar, B.F. Şenkal, Ö. Cankurtaran, Application of inverse gas chromatography in the surface characterization of diethanol amine modified polystyrene based polymer, Turk. J. Chem. 45 (2021) 1533–1542.
[146] C. Bilgiç, Determination of the surface properties of kaolinite by inverse gas chromatography, Water Sci. Technol. 2 (2017) 319–328.
[147] J. Yu, X. Lu, C. Yang, B. Du, S. Wang, Z. Ye, Inverse gas chromatography as a method for determination of surface properties of binding materials, Mater. Sci. Eng., A 242 (2017) 012001.
[148] T. Hamieh, Inverse gas chromatography to characterize the surface properties of solid materials, Chem. Mater. (2024), https://doi.org/10.1021/acs.chemmater.3c03091.
[149] T. Hamieh, J. Toufaily, A.B. Mouneimné, Effect of the tacticity of PMMA adsorbed on alumina and silica on the specific entropy change of polymer by inverse GC, Chromatographia 73 (2011) 99–107.
[150] T. Hamieh, Determination of acid base properties of poly(α-n-alkyl) methacrylates adsorbed on silica by inverse gas chromatography (IGC), Chromatographia 73 (2011) 709–719.
[151] B.P. Kumar, T. Hamieh, K.S. Pasupuleti, V.R. Pasupuleti, V.N. Rao, M.D. Kim, C. W. Kim, Surface thermal behavior and RT CO gas sensing application of an oligoacenaphthylene with p-hydroxyphenylacetic acid composite, ACS Omega 7 (41) (2022) 36307–36317.
[152] P.K. Basivi, V.R. Pasupuleti, T. Hamieh, Surface thermodynamic properties of sodium carboxymethyl cellulose by inverse gas chromatography, Chem. Eng. J. Adv. 9 (2022) 100207.
[153] P.K. Basivi, T.V.M. Sreekanth, R. Sivalingam, C.K. Thota, V.R. Pasupuleti, Surface characterization and London dispersive surface free energy of functionalized single-walled carbon nanotubes with a blend of polytetrafluoroethylene by inverse gas chromatography, Surf. Interface Anal. 51 (2019) 516–524.
[154] P. Reddi, Rani S. Ramanaiah, B. Praveen Kumar, K.S. Reddy, Lewis acid-base properties of cellulose acetate butyrate-poly (caprolactonediol) blend by inverse gas chromatography, Polym.-Plast. Technol. Eng. 52 (12) (2013) 1228–1234.
[155] B. Praveen Kumar, S. Ramanaiah, T.M. Reddy, K.S. Reddy, Surface thermodynamics of Efavirenz and a blend of Efavirenz with cellulose acetate propionate by inverse gas chromatography, Surf. Interface Anal. 48 (2016) 4–9.
[156] B. Praveen Kumar, S. Ramanaiah, T. Madhusudana Reddy, et al., Surface characterization of cellulose acetate propionate by inverse gas chromatography, Polym. Bull. 71 (2014) 125–132.
[157] A. Voelkel, J. Janas, J. Garcia-Dominguez, Inverse gas chromatography in characterization of surfactants: determination of binary parameter, J. Chromatogr. A 654 (1993) 135–141.
[158] A. Sudharshan Reddy, B. Praveen Kumar, S. Ramanaiah, K.S. Reddy, Surface thermodynamic properties of amberlite XAD-4 by inverse gas chromatography, Int. J. Polym. Anal. Char. 17 (2012) 278–290.
[159] T. Školáková, L. Souchová, J. Patera, M. Pultar, A. Školáková, P. Zámostný, Prediction of drug-polymer interactions in binary mixtures using energy balance supported by inverse gas chromatography, Eur. J. Pharmaceut. Sci. 130 (2019) 247–259.
[160] E. Petříková, J. Patera, O. Gorlová, Influence of active pharmaceutical ingredient structures on Hansen solubility parameters, Eur. J. Pharmaceut. Sci. 167 (2021) 106016.
[161] B. Strzemiecka, J. Kołodziejek, M. Kasperkowiak, A. Voelkel, Influence of relative humidity on the properties of examined materials by means of inverse gas chromatography, J. Chromatogr., A 1271 (2013) 201–206.
[162] S.C. Das, S.R. Behara, J.B. Bulitta, D.A. Morton, I. Larson, P.J. Stewart, Powder strength distributions for understanding de-agglomeration of lactose powders, Pharm. Res. (N. Y.) 29 (2012) 2926–2935.
[163] R. Ho, M. Naderi, J.Y.Y. Heng, D.R. Williams, F. Thielmann, P. Bouza, A.R. Keith, G. Thiele, D.J. Burnett, Effect of milling on particle shape and surface energy heterogeneity of needle-shaped crystals, Pharm. Res. (N. Y.) 29 (2012) 2806–2816.
[164] J.F. Gamble, M. Leane, D. Olusanmi, M. Tobyn, E. Supuk, J. Khoo, M. Naderi, Surface energy analysis as a tool to probe the surface energy characteristics of micronized materials—a comparison with inverse gas chromatography, Int. J. Pharm. 422 (2012) 238–244.
[165] Q. Zhou, D.A.V. David, Drug–lactose binding aspects in adhesive mixtures: controlling performance in dry powder inhaler formulations by altering lactose carrier surfaces, Adv. Drug Deliv. Rev. 64 (2012) 275–284.
[166] J. Kołodziejek, E. Główka, K. Hyla, A. Voelkel, J. Lulek, K. Milczewska, Relationship between surface properties determined by inverse gas chromatography and ibuprofen release from hybrid materials based on fumed silica, Int. J. Pharm. (Amst.) 441 (2013) 441–448.
[167] J.F. Gamble, R.N. Dave, S. Kiang, M.M. Leane, M. Tobyn, S.S.Y. Wang, Investigating the applicability of inverse gas chromatography to binary powdered systems: an application of surface heterogeneity profiles to understanding preferential probe-surface interactions, Int. J. Pharm. 445 (2013) 39–46.
[168] S.C. Das, I. Larson, D.A. Morton, P.J. Stewart, Determination of the polar and total surface energy distributions of particulates by inverse gas chromatography, Langmuir 27 (2) (2011) 521–523.
[169] S.C. Das, Q. Zhou, D.A. Morton, I. Larson, P.J. Stewart, Use of surface energy distributions by inverse gas chromatography to understand mechanofusion processing and functionality of lactose coated with magnesium stearate, Eur. J. Pharmaceut. Sci. 43 (2011) 325–333.
[170] Q. Zhou, J.A. Denman, T. Gengenbach, S. Das, L. Qu, H. Zhang, I. Larson, P. J. Stewart, D.A.V. Morton, Characterization of the surface properties of a model pharmaceutical fine powder modified with a pharmaceutical lubricant to improve flow via a mechanical dry coating approach, J. Pharmaceut. Sci. 100 (2011) 3421–3430.
[171] S.C. Das, P.J. Stewart, Characterizing surface energy of pharmaceutical powders by inverse gas chromatography at finite dilution, J. Pharm. Pharmacol. 64 (2012) 1337–1348.
[172] S. Das, I. Larson, P. Young, P. Stewart, Understanding lactose behavior during storage by monitoring surface energy change using inverse gas chromatography, Dairy Science Technologies. 90 (2–3) (2010) 271–285.
[173] D.J. Matthew, P. Young, D. Traini, The use of inverse gas chromatography for the study of lactose and pharmaceutical materials used in dry powder inhalers, Adv. Drug Deliv. Rev. 64 (2012) 285–293.
[174] H. Miyanishi, T. Nemoto, M. Mizuno, H. Mimura, S. Kitamura, Y. Iwao, S. Noguchi, S. Itai, Evaluation of crystallization behavior on the surface of nifedipine solid dispersion powder using inverse gas chromatography, Pharm. Res. (N. Y.) 30 (2013) 502–511.
[175] T. Hamieh, Determination of Lewis acid base properties of poly(α-n-alkyl) methacrylates adsorbed on silica by inverse GC, Chromatographia 73 (2011) 709–719.
[176] R. Ho, S.J. Hinder, J.F. Watts, S.E. Dilworth, D.R. Williams, J.Y.Y. Heng, Determination of surface heterogeneity of d-mannitol by sessile drop contact angle and finite concentration inverse gas chromatography, Int. J. Pharm. 387 (2010) 79–86.
[177] W. Wanga, Q. Hua, Y. Sha, D. Wu, S. Zheng, B. Liu, Surface properties of solid materials measured by modified inverse gas chromatography, Talanta 112 (2013) 69–72.
[178] S.C. Das, I. Larson, P. Young, P.J. Stewart, Understanding lactose behavior during storage by monitoring surface energy change using inverse gas chromatography, Dairy Sci. Technol. 90 (2010) 271–285.
[179] J. Kołodziejek, A. Voelkel, K. Heberger, Characterization of hybrid materials by means of inverse gas chromatography and chemometrics, J. Pharmaceut. Sci. 102 (2013) 1524–1531.
[180] B. Shi, D. Qi, A method for improving the calculation accuracy of acid–base constants by inverse gas chromatography, J. Chromatogr., A 1231 (2012) 73–76.
[181] M.D. Jones, P. Young, D. Traini, The use of inverse gas chromatography for the study of lactose and pharmaceutical materials used in dry powder inhalers, Adv. Drug Deliv. Rev. 64 (2012) 285–293.
[182] Tony) Qi Zhou, M.A.V. David, Advances in solid formulation of pharmaceutical biologics, Adv. Drug Deliv. Rev. 175 (2021) 113827.
[183] L. Bilancetti, D. Poncelet, C. Loisel, S. Mazzitelli, C. Nastruzzi, A statistical approach to optimize the spray drying of starch particles : application to dry powder coating, AAPS PharmSciTech 11 (2010) 1257–1267.
[184] J. Brum, D. Burnett, Quantification of surface amorphous content using dispersive surface energy: the concept of effective amorphous surface area, AAPS PharmSciTech 12 (2011) 887–892.
[185] D.J. Burnett, J. Khoo, M. Naderi, J.Y.Y. Heng, G.D. Wang, F. Thielmann, Effect of processing route on the surface properties of amorphous indomethacin measured by inverse gas chromatography, AAPS PharmSciTech 13 (2012) 1511–1517.
[186] P. Ke, S. Hasegawa, H. Al-Obaidi, G. Buckton, Investigation of preparation methods on surface/bulk structural relaxation and glass fragility of amorphous solid dispersions, Int. J. Pharm. 422 (2012) 170–178.
[187] V.N. Le, H. Bierend, E. Robins, H. Steckel, M.P. Flament, Influence of the lactose grade within dry powder formulations of fluticasone propionate and terbutaline sulphate, Int. J. Pharm. 422 (2012) 75–82.

[188] R. Ho, A.S. Muresan, G.A. Hebbink, J.Y.Y. Heng, Influence of fines on the surface energy heterogeneity of lactose for pulmonary drug delivery, Int. J. Pharm. 388 (2010) 88–94.
[189] M.H. Shariare, M. de Matas, P. York, Q. Shao, The impact of material attributes and process parameters on the micronisation of lactose monohydrate, Int. J. Pharm. 408 (2011) 58–66.
[190] H. Miyanishi, T. Nemoto, M. Mizuno, H. Mimura, S. Kitamura, Y. Iwao, S. Noguchi, S. Itai, Evaluation of crystallization behavior on the surface of nifedipine solid dispersion powder using inverse gas chromatography, Pharm. Res. (N. Y.) 30 (2013) 502–511.
[191] Y. Peng, D.J. Gardner, Y. Han, Z. Cai, M.A. Tshabalala, Influence of drying method on the surface energy of cellulose nanofibrils determined by inverse gas chromatography, J. Colloid Interface Sci. 405 (2013) 85–95.
[192] R. Kolakovic, L. Peltonen, A. Laukkanen, J. Hirvonen, T. Laaksonen, Nanofibrillar cellulose for controlled drug delivery, Eur. J. Pharm. Biopharm. 82 (2013) 308–315.
[193] T. Tay, S. Das, P. Stewart, Magnesium stearate increases salbutamol sulphate dispersion: what is the mechanism? Int. J. Pharm. 383 (2010) 62–69.
[194] X. Han, L. Jallo, D. To, C.Y. Ghoroi, R. Dave, Passivation of high-surface-energy sites of milled ibuprofen crystals via dry coating for reduced cohesion and improved flowability, J. Pharmaceut. Sci. 102 (2013) 2282.
[195] B.P. Kumar, P.R. Rani, T.M.S. Reddy, K.S. Reddy, Surface Characterization of Phenylpropanolamine Drug by Inverse Gas Chromatography. ISRN Physical Chemistry, vol. 142687, 2013, pp. 1–5.
[196] B.P. Kumar, T.M. Reddy, K.S. Reddy, Surface characterization of 2-hydroxypyrimidine sulphate by inverse gas chromatography, J. Pharmaceutical Investigation. 44 (2014) 9–14.
[197] B.P. Kumar, V.R. Pasupuleti, S. Ramanaiah, T.M.S. Reddy, K.S. Reddy, S.J. Park, Inverse gas chromatography study on London dispersive surface free energy and electron acceptor–donor of fluconazole drug, J. Chem. Eng. Data 62 (7) (2017) 2090–2094.
[198] E. Özge, C. Hasçiçek, Preparation and evaluation of comparison- coated tablets for chrono pharmaceutical drug delivery, J. Fac. Pharm. Ankara. 47 (2) (2023) 508–519.
[199] A. Vidal, E. Papirer, W.M. Jaio, J.B. donnet, Modification of silica surfaces by grafting of alkyl chains. I — characterization of silica surfaces by inverse gas-solid chromatography at zero surface coverage, Chromatographia 23 (1987) 121–128.
[200] E. Fekete, J. Móczó, B. Pukánszky, Determination of the surface characteristics of particulate fillers by inverse gas chromatography at infinite dilution: a critical approach, J. Colloid Interface Sci. 269 (2004) 143–152.
[201] D.S. Keller, P. Luner, Surface energetics of calcium carbonates using inverse gas chromatography, Colloids Surf. A Physicochem. Eng. Asp. 161 (2000) 401–415.
[202] E. Díaz, S. Ordóñez, A. Vega, J. Coca, Evaluation of adsorption properties of zeolites using inverse gas chromatography: comparison with immersion calorimetry, Thermochim. Acta 434 (2005) 9–14.
[203] B. Strzemiecka, J. Kołodziejek, M. Kasperkowiak, A. Voelkel, Influence of relative humidity on the properties of examined materials by means of inverse gas chromatography, J. Chromatogr. A 1271 (2012) 201–206.
[204] B. Strzemiecka, A. Voelkel, M. Kasperkowiak, Characterization of zeolites as potential new generation fillers in abrasive articles. Physico chemical properties of zeolites and their interactions with resins, Colloids Surf. A Physicochem. Eng. Asp. 372 (2010) 80–85.
[205] M. Kasperkowiak, J. Kołodziejek, B. Strzemiecka, A. Voelkel, Effect of impregnating agent and relative humidity on surface characteristics of sorbents determined by inverse gas chromatography, J. Chromatogr. A 1288 (2013) 101–104.
[206] B. Strzemiecka, M. Kasperkowiak, M. Łożyński, D. Paukszta, A. Voelkel, Examination of zeolites as fragrance carriers, Microporous Mesoporous Mater. 161 (2012) 106–114.
[207] S. Katz, D.G. Gray, The adsorption of hydrocarbons on cellophane: I. Zero coverage limit, J. Colloid Interface Sci. 82 (1981) 318–325.
[208] F. Thielmann, D. Butler, D. Williams, E. Baumgarten, Characterization of microporous materials by dynamic sorption methods, Stud. Surf. Sci. Catal. 129 (2000) 633–638.
[209] R. Menzel, A. Lee, A. Bismarck, M.S. Shaffer, Inverse gas chromatography of as received and modified carbon nanotubes, Langmuir 25 (2009) 8340–8348.
[210] S. Yang-hsin, L. Mei-syue, Adsorption of selected volatile organic vapors on multiwall carbon nanotubes, J. Hazard Mater. 154 (2008) 21–28.
[211] S. Xie, E. Suuberg, Adsorption of trichloroethylene on common indoor materials studied using a combined inverse gas chromatography and frequency response technique, J. Chromatogr., A 1669 (2022) 462926.
[212] K. Yusuf, A. Natraj, K. Li, M. Ateia, Z.A. Alothman, W.R. Dichtel, Inverse gas chromatography demonstrates the crystallinity-dependent physicochemical properties of two-dimensional covalent organic framework stationary phases, Chem. Mater. 35 (2023) 1691–1701.
[213] A.A. Kotova, D. Thiebaut, J. Vial, A. Tissot, C. Serre, Metal-organic frameworks as stationary phases for chromatography and solid phase extraction: a review, Coord. Chem. Rev. 167 (2022) 214364.
[214] H. Saini, E. Otyepkov, A. Schneemann, R. Zboril, M. Otyepka, A.R. Fischer, K. Jayaramulu, Hierarchical porous metal–organic framework materials for efficient oil–water separation, J. Mater. Chem. A 10 (2022) 2751–2785.
[215] C. Singh, S. Mukhopadhyay, I. Hod, Metal–organic framework derived nanomaterials for electrocatalysis: recent developments for CO_2 and N_2 reduction, Nano Convergence 8 (2021) 1–10.
[216] K. Yusuf, O. Shekhah, Z.A. Alothman, M. Eddaoudi, Metal-organic frameworks characterization via inverse pulse gas chromatography, Appl. Sci. 11 (2021) 10243.
[217] T.H. Rupam, T. Steenhaut, M.L. Palash, Y. Filinchuk S. Hermans, B.B. Saha, Thermochemical energy applications of green transition metal doped MIL–100 (Fe), Chem. Eng. J. 448 (2022) 137590.
[218] T. Hamieh, A.A. Jrad, T.R. Carmes, M. Hmadeh, J. Toufaily, Surface thermodynamics and Lewis acid-base properties of metal-organic framework Crystals by Inverse gas chromatography at infinite dilution, J. Chromatogr., A 1666 (2022) 462849.
[219] K. Yusuf, O. Shekhah, Z.A. Alothman, M. Eddaoudi, Metal-organic frameworks characterization via inverse pulse gas chromatography, Appl. Sci. 11 (2021) 10243.
[220] W.A. Mustafa, M.M.M.A. Kader, A review of histogram equalization techniques in image enhancement application, J. Phys. Conf. Ser. 1019 (2018) 012026.
[221] S. Julian, R.A.J. Woolley, P. Moriarty, Scanning probe image wizard: a toolbox for automated scanning probe microscopy data analysis, Rev. Sci. Instrum. 84 (2013) 113701.
[222] O. Queen, G.A. McCarver, S. Thatigotla, B.P. Abolins, C.L. Brown, V. Maroulas, K. D. Vogiatzis, Polymer graph neural networks for multitask property learning, npj Comput. Mater. 9 (1) (2023) 1–10, 90.
[223] P.H.H. Araújo, C. Sayer, J.C. De la Cal, J.M. Asua, E.L. Lima, J.C. Pinto, Utilization of neural networks as soft sensors to monitor emulsion polymerization reactions (average particle diameter and conversion), Lat. Am. Appl. Res. 31 (2001) 525–531.
[224] J. Deng, G. Jia, Dielectric constant prediction of pure organic liquids and their mixtures with water based on interpretable machine learning, Fluid Phase Equil. 561 (2022) 113545.
[225] R. Houhou, T. Bocklitz, Trends in artificial intelligence, machine learning, and chemometrics applied to chemical data, Analytical Science Advances 2 (3–4) (2021) 128–141.
[226] Z. Dai, F. Shi, B. Zhang, M. Li, Z. Zhang, Effect of sizing on carbon fiber surface properties and fibers/epoxy interfacial adhesion, Appl. Surf. Sci. 257 (15) (2011) 6980–6985.
[227] L.P. Barron, G.L. McEneff, Gradient liquid chromatographic retention time prediction for suspect screening applications: a critical assessment of a generalized artificial neural network-based approach across 10 multi-residue reversed-phase analytical methods, Talanta 147 (2016) 261–270.
[228] J. Nistane, L. Chen, Y. Lee, R. Lively, R. Ramprasad, Estimation of the Flory-Huggins interaction parameter of polymer-solvent mixtures using machine learning, MRS Communications (2022) 1–7.
[229] K.M. Toots, S. Sild, J. Leis, W.E. Acree Jr., U. Maran, Machine learning quantitative structure–property relationships as a function of ionic liquid cations for the gas-ionic liquid partition coefficient of hydrocarbons, Int. J. Mol. Sci. 23 (14) (2022) 7534.
[230] N. Pouyanfar, S.Z. Harofte, M. Soltani, S. Siavashy, E. Asadian, F. Ghorbani-Bidkorbeh, R. Keçili, C.M. Hussain, Artificial intelligence-based microfluidic platforms for the sensitive detection of environmental pollutants: recent advances and prospects, Trends in Environmental Analytical Chemistry (2022) 00160.
[231] R.M. Aghav, S. Kumar, S.N. Mukherjee, Artificial neural network modeling in competitive adsorption of phenol and resorcinol from water environment using some carbonaceous adsorbents, J. Hazard Mater. 188 (1–3) (2011) 67–77.
[232] H. Kinnunen, G. Hebbink, H. Peters, J. Shur, R. Price, Defining the critical material attributes of lactose monohydrate in carrier based dry powder inhaler formulations using artificial neural networks, AAPS PharmSciTech 15 (2014) 1009–1020.
[233] A. Niederquell, N. Wyttenbach, M. Kuentz, New prediction methods for solubility parameters based on molecular sigma profiles using pharmaceutical materials, Int. J. Pharm. 546 (1–2) (2018) 137–144.
[234] W. Zheng, Z. Ma, W. Sun, L. Zhao, Target high-efficiency ionic liquids to promote H2SO4-catalyzed C4 alkylation by machine learning, AIChE J. 68 (7) (2022) 17698.
[235] T. Bo, C. Yang, J. Liu, H. Zhang, Artificial intelligence-based SDA technology improves the deasphalting effect and mechanism of inferior solvents, in: Signal and Information Processing, Networking and Computers: Proceedings of the 9th International Conference on Signal and Information Processing, Networking and Computers (ICSINC), Springer Nature Singapore, Singapore, 2022, pp. 1155–1164.
[236] J. Szoplik, P. Muchel, Using an artificial neural network model for natural gas compositions forecasting, Energy 263 (2023) 126001.
[237] L. Wei, F.A. Wang, Y. Liu, Y. Chai, LB energy-saving high temperature shift catalyst and its adsorption thermodynamics, Kor. J. Chem. Eng. 26 (2009) 42–47.
[238] G. Wang, T. Briskot, T. Hahn, P. Baumann, J. Hubbuch, Estimation of adsorption isotherm and mass transfer parameters in protein chromatography using artificial neural networks, J. Chromatogr. A 1487 (2017) 211–217.
[239] S. Sremac, A. Popović, Ž. Todorović, Đ. Čokeša, A. Onjia, Interpretative optimization and artificial neural network modeling of the gas chromatographic separation of polycyclic aromatic hydrocarbons, Talanta 76 (1) (2008) 66–71.
[240] K. Brudzewski, A. Kesik, K. Kołodziejczyk, U. Zborowska, J. Ulaczyk, Gasoline quality prediction using gas chromatography and FTIR spectroscopy: an artificial intelligence approach, Fuel 85 (4) (2006) 553–558.
[241] Z. Giuseppe, G. Manuela, B. Marta, G. Vincenzo, Application of artificial neural network on mono-and sesquiterpenes compounds determined by headspace solid-phase microextraction–gas chromatography–mass spectrometry for the Piedmont ricotta cheese traceability, J. Chromatogr. A 1071 (1–2) (2005) 247–253.

[242] S. Squara, A. Caratti, A. Fina, E. Liberto, N. Spigolon, G. Genova, G. Castello, I. Cincera, C. Bicchi, C. Cordero, Artificial Intelligence decision-making tools based on comprehensive two-dimensional gas chromatography data: the challenge of quantitative volatilomics in food quality assessment, J. Chromatogr. A 1700 (2023) 464041.
[243] T.L. Liu, L.Y. Liu, F. Ding, Y.Q. Li, A machine learning study of polymer-solvent interactions, Chin. J. Polym. Sci. 40 (7) (2022) 834–842.
[244] C.A. Bergström, C.M. Wassvik, U. Norinder, K. Luthman, P. Artursson, Global and local computational models for aqueous solubility prediction of drug-like molecules, J. Chem. Inf. Comput. Sci. 44 (4) (2004) 1477–1488.
[245] L. Tao, J. He, T. Arbaugh, J.R. McCutcheon, Y. Li, Machine learning prediction on the fractional free volume of polymer membranes, J. Membr. Sci. 665 (2023) 121131.